3-D Structure of the Variscan Thrust Front in Northern France: New Insights From Seismic Reflection Profiles

A. Laurent, Olivier Averbuch, Laurent Beccaletto, Fabien Graveleau, Frédéric Lacquement, Laure Capar, Stéphane Marc

▶ **To cite this version:**

A. Laurent, Olivier Averbuch, Laurent Beccaletto, Fabien Graveleau, Frédéric Lacquement, et al.. 3-D Structure of the Variscan Thrust Front in Northern France: New Insights From Seismic Reflection Profiles. Tectonics, 2021, 40 (7), 10.1029/2020TC006642 . hal-04337843

HAL Id: hal-04337843
https://hal.science/hal-04337843v1

Submitted on 14 Dec 2023

HAL is a multi-disciplinary open access archive for the deposit and dissemination of scientific research documents, whether they are published or not. The documents may come from teaching and research institutions in France or abroad, or from public or private research centers.

L'archive ouverte pluridisciplinaire **HAL**, est destinée au dépôt et à la diffusion de documents scientifiques de niveau recherche, publiés ou non, émanant des établissements d'enseignement et de recherche français ou étrangers, des laboratoires publics ou privés.

Copyright

Check for updates

Tectonics

RESEARCH ARTICLE
10.1029/2020TC006642

3-D Structure of the Variscan Thrust Front in Northern France: New Insights From Seismic Reflection Profiles

A. Laurent[1], O. Averbuch[1], L. Beccaletto[2], F. Graveleau[1], F. Lacquement[2], L. Capar[2], and S. Marc[2]

[1]Univ. Lille, CNRS, Univ. Littoral Côte d'Opale, UMR 8187-LOG-Laboratoire d'Océanologie et de Géosciences, Lille, France, [2]BRGM, Orléans, France

Key Points:

- Seismic data emphasize the large underthrusting of the Carboniferous foreland basin beneath the northern France Variscan thrust wedge
- 3-D imaging of the main thrust Allochton Main Basal Thrust evidences a major lateral ramp segmenting the frontal thrust zone
- Inherited normal faults from the Laurussian margin exerted a major control on the dynamics and segmentation of the thrust front

Correspondence to:
A. Laurent,
aurore.laurent@univ-lille.fr

Citation:
Laurent, A., Averbuch, O., Beccaletto, L., Graveleau, F., Lacquement, F., Capar, L., & Marc, S. (2021). 3-D structure of the Variscan thrust front in northern France: New insights from seismic reflection profiles. *Tectonics*, *40*, e2020TC006642. https://doi.org/10.1029/2020TC006642

Received 11 DEC 2020
Accepted 16 JUN 2021

© 2021. American Geophysical Union. All Rights Reserved.

Abstract In NW Europe, the late Carboniferous Variscan collision between the Laurussia and the Armorica-Gondwana continental blocks led to the development of a crustal-scale north-verging thrust system along the southern Laurussian margin. In northern France, the 3-D geometry and kinematics of the Variscan deformation front have been investigated on the basis of reprocessing and interpreting 532 km of industry-level seismic reflection profiles. This extensive seismic imaging provides new constraints on the structural and kinematic features of the orogenic front. It particularly emphasizes the localization of displacement along the main frontal thrust zone that accommodated more than 50 km of total displacement of the allochthonous units above the foreland. It also highlights the induced large underthrusting of the foreland basin below the frontal thrust zone, and its truncation in a general out-of-sequence mode of thrust propagation. We built structural maps that led to better delineating a major NW-SE lateral ramp along the main frontal thrust. The Mid-Upper Devonian series within the flexured foreland were deformed at depth by N060–080° trending and N110–130° trending syn-sedimentary normal faults that led to their south-to southwestward thickening. These pre-existing structures along the margin have exerted a primary control on the ensuing dynamics and geometry of the Northern Variscan Front by localizing both the frontal and lateral ramps during thrust wedge growth.

1. Introduction

Mountain fronts and foreland basins have been extensively studied in the past 50 years (e.g., Nemcok et al., 2005; Lacombe et al., 2007; Poblet & Lisle, 2011; Hammerstein et al., 2020 and references herein). They provide a record of the kinematic history of thrust propagation into the foreland, as well as of the orogenic relief erosion (e.g., Allen et al., 1986; Vann et al., 1986; DeCelles & Giles, 1996; Ziegler et al., 2002; Ford, 2004; Ortner et al., 2015). The dynamics of mountain-belt formation has been investigated in the frame of the accretionary wedge model that compares (for good mechanical reasons) the formation of a mountain belt with a pile of gravels pushed by a moving bulldozer (Chapple, 1978; Dahlen et al., 1984; Davis et al., 1983). Additionally, the style of deformation propagation of the thrust front within the foreland has been often investigated either in a first-order thin-skinned or a thick-skinned mode (e.g., Bally et al., 1966; Dahlstrom, 1969; Boyer & Elliott, 1982; Butler, 1987; Lacombe & Mouthereau, 2002), depending on the effect of basement structure on the deformed cover in the orogenic wedge.

One of the main parameters controlling the structural diversity of a foldbelt front is the rheology of the foreland rocks. Changes in the mechanical coupling between the propagating thrust wedge and its foreland sequence, along with regional structural inheritance (pre-existing basement faults and 3-D configuration of décollements) exert a primary control on the evolution of mountain-belts (e.g., Butler, 1989; Moore, 1989; Huiqi et al., 1992; Gutscher et al., 1996; Kley et al., 1999; Ziegler et al., 2002; Lacquement et al., 2005; Butler et al., 2006; Ravaglia et al., 2006). The importance of mechanical stratigraphy and structural inheritance has been demonstrated in numerous mountains fronts (e.g., Fitz-Diaz et al., 2011; Butler et al., 2018; Legeay et al., 2020) and by different analog and numerical modeling approaches (e.g., Ravaglia et al., 2006; Graveleau et al., 2012; Hughes, 2020). Surface processes (erosion and sedimentation) are also important factors controlling the structural evolution of mountain belts (Fillon et al., 2013; Konstantinovskaya & Malavieille, 2005; Malavieille, 2010; Storti & McClay, 1995) because they determine the sedimentary fluxes between the hinterland and the foreland. As a result of these heterogeneities in foreland rheological properties and changes in erosion and sedimentation rates, a large diversity of 3-D geometries and kinematics

19449194, 2021, 7, Downloaded from https://agupubs.onlinelibrary.wiley.com/doi/10.1029/2020TC006642 by Cochrane France, Wiley Online Library on [13/12/2023]. See the Terms and Conditions (https://onlinelibrary.wiley.com/terms-and-conditions) on Wiley Online Library for rules of use; OA articles are governed by the applicable Creative Commons License

can be observed in fold-and-thrust belts. It includes for examples triangle zones, buried thrust fronts, in-sequence versus out-of-sequence thrusting, duplexes, fore-versus back-thrusting, folding versus faulting, etc (e.g., Jones, 1982; Banks & Warburton, 1986; Price, 1986; Vann et al., 1986; Morley, 1986, 1988; Averbuch et al., 1995; Tozer et al., 2006; Ortner et al., 2015; Von Hagke & Malz, 2018).

Mountain fronts represent also a very privileged target for the exploration and exploitation of natural resources because subsidence of the foreland basin associated to the combined effects of thrusting and syn-orogenic sedimentation, have allowed the development, migration and trapping of hydrocarbons (Lacombe et al., 2007; McClay, 2004; Needham et al., 2004; Nemcok et al., 2005). Recently, studies of foreland basin geology found also some additional applications for renewable energy and particularly geothermal energy. Thus, high temperature waters have been investigated and drilled in reservoirs buried a few kilometers in foreland basins. This is the case in the Alps, where temperatures reach about 80–140°C under the molassic foreland basin in Germany (Farquharson et al., 2016), or along the fossil Variscan belt of northern Europe, where warm waters around 60–70°C are exploited in southern Belgium (Delmer et al., 1982; Licour, 2012).

In order to gain insights on foreland fold-and-thrust belt dynamics, we investigated the geometry and kinematics of the Northern Variscan Front in northern France. This mountain front is an ancient, deeply eroded fold-and-thrust belt that was active 300 Ma ago. Our study is based on the interpretation of 532 km of reprocessed seismic reflection profiles covering a 5,130 km^2 area. The various orientations of the seismic profiles allow to intersect the main regional structural features and to build for the first time a comprehensive 3-D view of this portion of the Northern Variscan thrust front. Results highlight the geometry of a major lateral ramp segmenting the main frontal thrust. They also emphasize the control of structural inheritance (normal faults) of the underthrust margin on the deformation pattern of the thrust wedge.

2. Geological Setting

2.1. Outline of the Devonian-Carboniferous Geodynamic Evolution in Northern France

The late Paleozoic geodynamics of northern France was controlled by the growth of the Variscan mountain belt, a major orogenic system that extends across several thousands of kilometers across Europe (Figure 1). The Variscan orogen resulted from a polyphased collisional process between the Laurussia and Gondwana paleocontinents from Mid-Devonian (ca 380 Ma) to late Carboniferous times (ca 305 Ma). This accounted for the progressive closure of a complex set of interacting oceanic basins and the accretion of microcontinents (e.g., Matte, 2001; Franke, 2006; Ballèvre et al., 2009). The northern deformation front corresponds to the inverted southern Laurussian margin (Figure 1).

The latter was primarily structured during a major rifting phase from Early (Lochkovian) to Middle Devonian (Eifelian) that resulted in the opening of a relatively narrow oceanic realm called the Rheno-Hercynian Ocean (Franke, 1992, 2000; Franke et al., 1995; Meilliez et al., 1991; Oncken et al., 2000; Shail & Leveridge, 2009). The Rheno-Hercynian oceanic basin is considered to have formed in a back-arc tectonic setting above the north-verging subducting slab of the South Armorican-Moldanubian Ocean (Averbuch & Piromallo, 2012; Cobert et al., 2018; Franke, 1992; Franke et al., 1995; Golonka, 2020; Oncken et al., 1999; Shail & Leveridge, 2009; Ziegler, 1989).

Extensional deformation, although of lesser importance than during the rifting stage, persisted until the end of the Devonian (Famennian) as demonstrated by tectono-sedimentary studies in the Belgian Ardennes (Préat & Boulvain, 1988; Thorez & Dreesen, 1986) and in southern England (Leveridge, 2011; Shail & Leveridge, 2009). The southern Laurussian margin was dissected by a series of N50–70° and N110–130° striking normal faults that delimited the Dutch-Belgian Brabant continental high along its south-eastern and south-western borders (Meilliez et al., 1991; Smit et al., 2018; Van Hulten, 2012). During the syn-rift subsidence, thick Lower Devonian siliciclastics sediments were deposited in the distal part of the Laurussian margin (Ardennes, Rhenish Slate belt) (Figure 2). During the post-rift phase that lasted from Mid-Late Devonian to early Carboniferous times, a large-scale transgressive carbonate platform formed above the slowly subsiding Laurussian margin and Brabant basement high (Figure 2).

During the Late Devonian and Mississippian, a general N–S convergence caused the gradual closure of the Rheno-Hercynian Ocean by southward subduction beneath the Armorican-Saxothuringian block (Averbuch

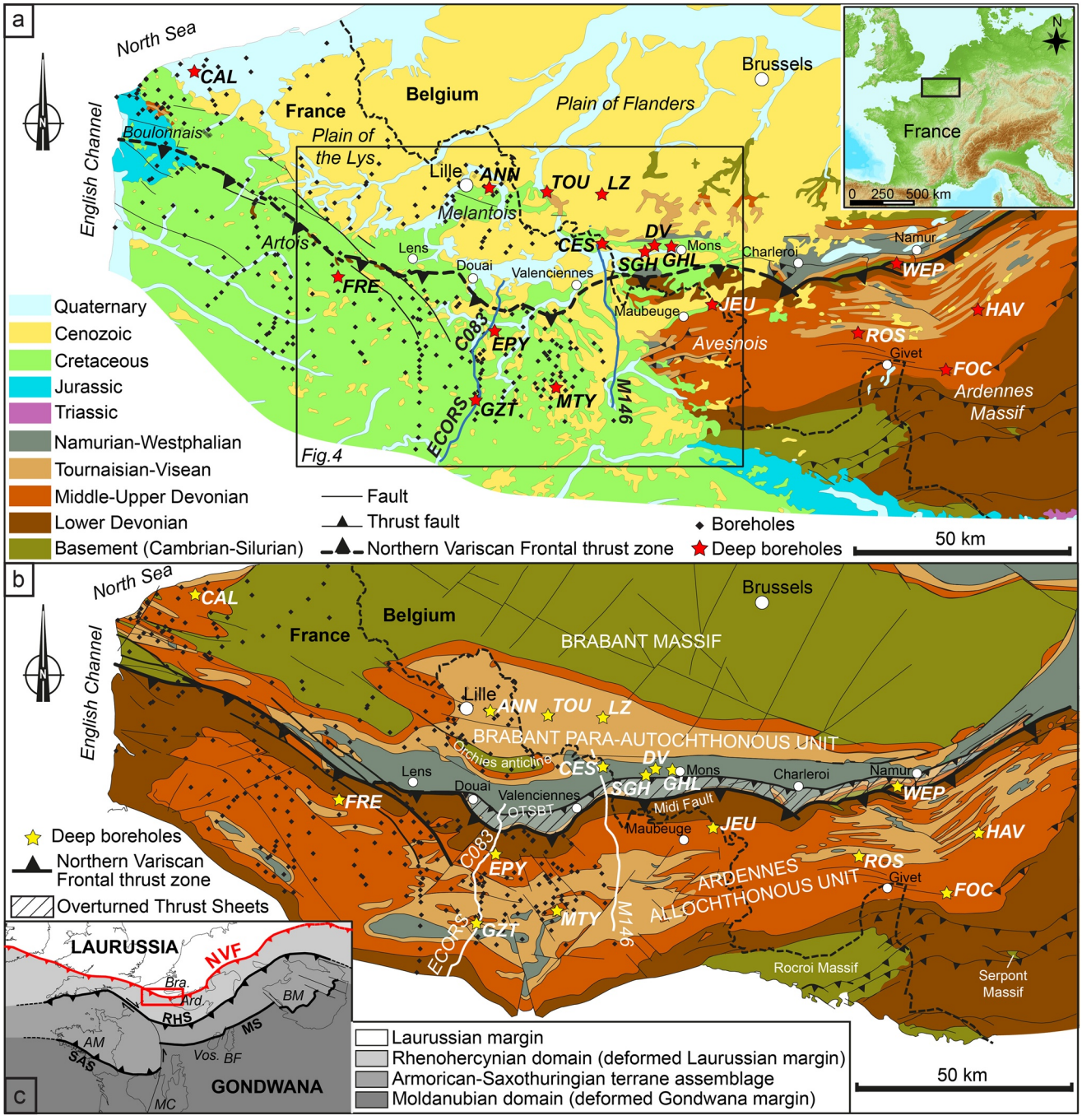

Figure 1. (a) Simplified geological map of northern France-southern Belgium (modified from the geological map of France, scale 1:1,000,000, Chantraine et al., 2003). The black frame corresponds to the location of Figure 4. (b) Structural map of the Variscan basement in northern France-southern Belgium (modified from C.F.P. et al., 1965 and Averbuch et al., 2004). This map is based on outcrop, well and geophysical data. The location of the Northern Variscan Front is based on previous studies. Borehole legend: ANN: Annappes; CAL: Calais; CES: Condé-sur-l'Escaut; DV: Douvrain; EPY: Epinoy; FOC: Focant; FRE: Frevillers; GHL: Ghlin; GZT: Gouzeaucourt; HAV: Havelange; JEU: Jeumont; LZ: Leuze; MTY: Montigny-en-Cambrésis; ROS: Rosières; SGH: Saint-Ghislain; TOU: Tournai; WEP: Wépion. c. Sketch map of the Variscan orogenic system in NW Europe (modified from Guillot et al., 2020). NVF: Northern Variscan deformation front; MS: Moldanubian suture; RHS: Rhenohercynian suture; SAS: South Armorican suture; AM: Armorican Massif; Ard.: Ardennes; BF: Black Forest; BM: Bohemian Massif; Bra. Brabant Massif; MC: Massif Central; Vos.: Vosges.

19449194, 2021, 7, Downloaded from https://agupubs.onlinelibrary.wiley.com/doi/10.1029/2020TC006642 by Cochrane France, Wiley Online Library on [13/12/2023]. See the Terms and Conditions (https://onlinelibrary.wiley.com/terms-and-conditions) on Wiley Online Library for rules of use; OA articles are governed by the applicable Creative Commons License

10.1029/2020TC006642

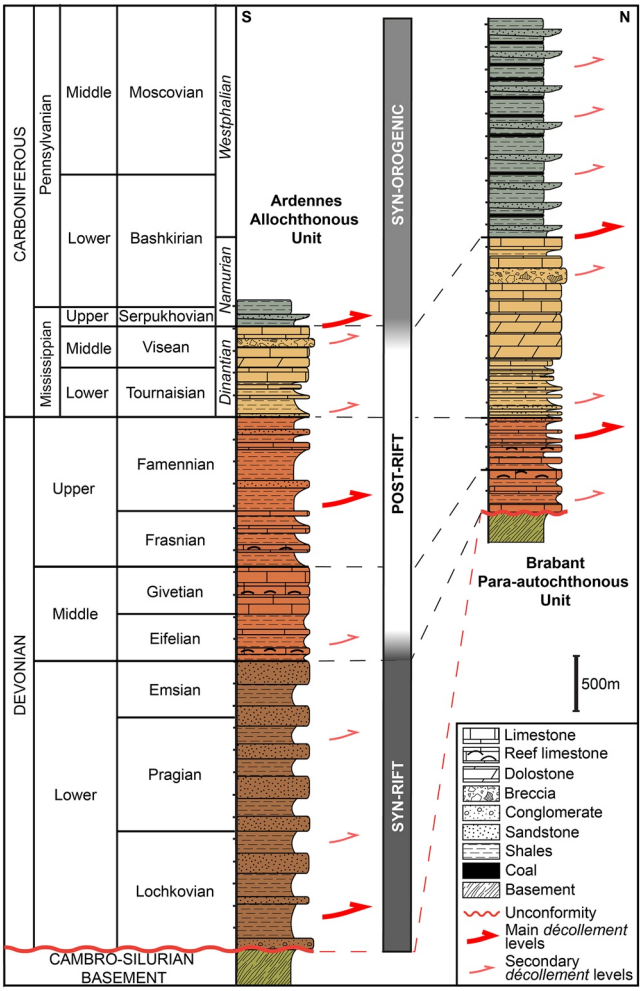

Figure 2. Synthetic lithostratigraphic logs of the Ardennes Allochthonous Unit and the Brabant Para-autochthonous Unit in northern France-southern Belgium. The thicknesses are based on data from deep boreholes in the region (see Figure 1).

& Piromallo, 2012; Cazes et al., 1985; Franke et al., 2017; Golonka, 2002; Golonka & Gaweda, 2012) (Figure 1). Starting from the middle Visean times onwards (ca 340 Ma), this ultimately led to the collision of Laurussia with the Armorica-Gondwana accretionary complex (e.g., Schulmann et al., 2002; Guillot et al., 2020). The Variscan collision stage is characterized by an overall NNW-SSE shortening (e.g., Corfield et al., 1996; Oncken et al., 2000; Averbuch et al., 2004; Averbuch & Piromallo, 2012) that was responsible for the tectonic inversion of the southern Laurussian margin. This resulted in the formation of a crustal-scale north-verging thrust system that propagated outward from the Late Mississippian (Visean) to the Middle Pennsylvanian (Westphalian) (Cazes et al., 1985; Fielitz and Mansy, 1999; Franke, 2000; Oncken et al., 2000; Plesch and Oncken, 1999). Tectonic stresses exerted on the lithosphere by the continental subduction and the increasing orogenic load led to flexural bending of the Laurussian continental lithosphere (e.g., Karner & Watts, 1983) and to the formation of a large-scale foredeep along the Northern Variscan Front. The latter can be tracked from Ireland to Northern Germany (Burgess & Gayer, 2000; Oncken et al., 2000; Plesch & Oncken, 1999; Tanner et al., 2011) and is likely to extend eastward to SE Poland (Lublin basin area) through a major bend along the Teisseyre-Tornquist zone (Krzywiec et al., 2017; Mazur et al., 2020) (Figure 1c). In northern France and southern Belgium, this foredeep was filled with up to 3.5 kilometers of synorogenic, coal-bearing, deposits during the Late Mississippian-Middle Pennsylvanian (Namurian-Westphalian 325–305 Ma) (Becq-Giraudon, 1983; Bouroz, 1969; Delmer et al., 2001) (Figure 2).

2.2. Basic Structural Features of the Northern Variscan Thrust Front in Northern France

In northern France, the Northern Variscan Front is almost never visible at the surface because it is covered by 100-to-200 meters of unconformable Mid-Cretaceous to Eocene sedimentary layers (Figure 1a). Apart from scarce outcrops of Paleozoic rocks exhumed in the Boulonnais and Artois hills resulting from Tertiary uplift (Mansy et al., 2003; Minguely et al., 2010), the most prominent outcrops of Paleozoic substratum are found in the Ardennes Massif and the Avesnois region. The Northern Variscan Front was discovered and extensively studied during the 19th–20th centuries during the intensive coal-mining activity. These first exploration data allowed to draw a general map of the thrust front at depth showing that its strike varies progressively from WNW-ESE (N110–120°) in the Boulonnais and Artois regions to ENE-WSW (N60–70°) in the Avesnois region and the Ardennes Massif (i.e., the classical V-shape of the Variscan belt) (Figures 1b and 1c). Some second-order trend changes have been defined in this general structural framework, such as the reentrant to the south of Douai and Valenciennes in the French coal-basin district.

The deep structure of the thrust wedge remained poorly known until new geophysical data (mainly seismic reflection profiles) and exploration wells were acquired during the 1980's by the ECORS program and hydrocarbons exploration (Cazes et al., 1985; Le Gall, 1992; Raoult, 1986, 1988; Raoult & Meilliez, 1987). These data considerably improved the knowledge on the deep structure of this orogenic front and showed the first-order geometry of the fold-thrust system. More recently, reprocessing and interpretation of a selected seismic profile (M146) along the French-Belgian border (Averbuch et al., 2018; Lacquement, 2001; Lacquement et al., 1999; Mansy et al., 1997) allowed to better define these first observations and better characterize the current structural model of the thrust front, as illustrated in Figures 1b and 3.

The structure of the thrust front in northern France and southern Belgium is classically subdivided into four major tectonic units (Figures 1b and 3a). In the following parts of our text, and essentially based on

19449194, 2021, 7, Downloaded from https://agupubs.onlinelibrary.wiley.com/doi/10.1029/2020TC006642 by Cochrane France, Wiley Online Library on [13/12/2023]. See the Terms and Conditions (https://onlinelibrary.wiley.com/terms-and-conditions) on Wiley Online Library for rules of use; OA articles are governed by the applicable Creative Commons License

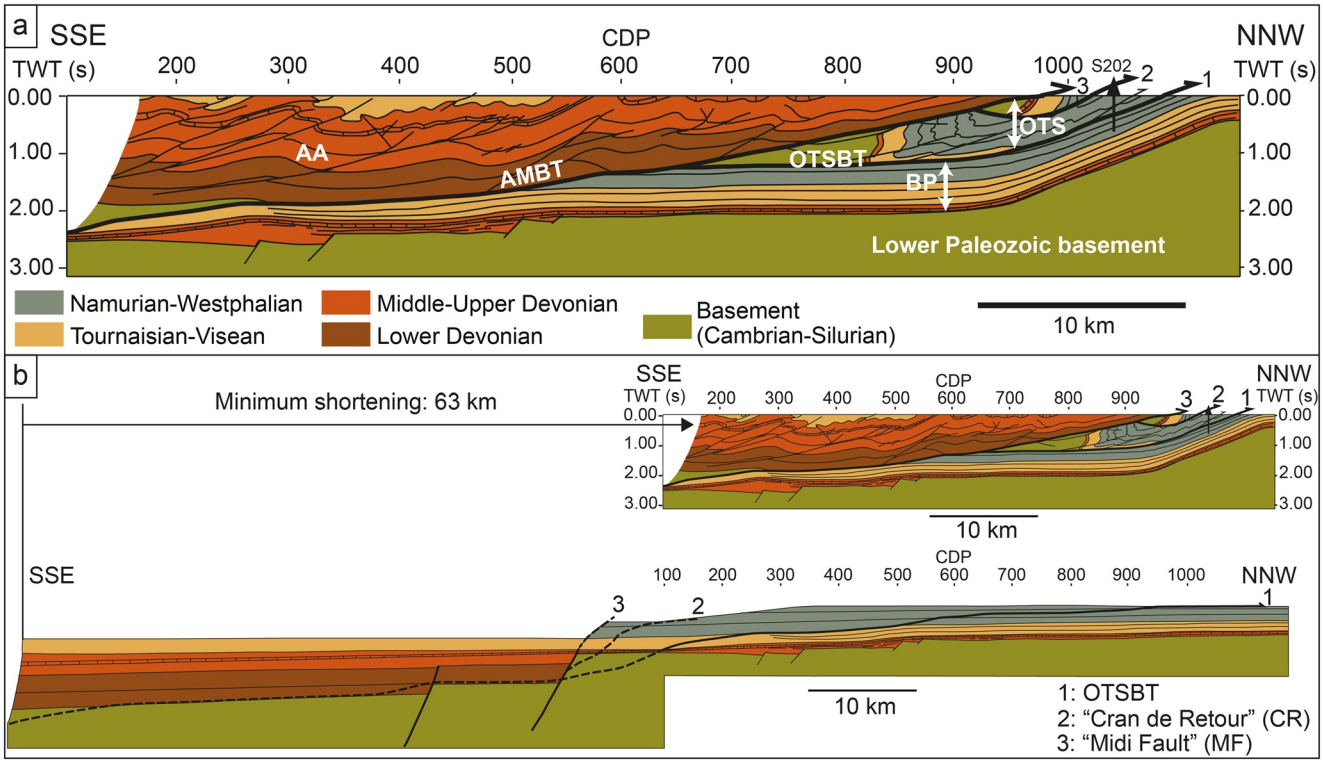

Figure 3. (a) Balanced cross-section along the M146 seismic profile in the area of Valenciennes (location in Figure 1b) illustrating the main structural features of the thrust front. Modified from Lacquement et al. (1999) and Mansy & Lacquement (2006). AA: Ardennes Allochthonous Unit, AMBT: Allochthon Main Basal Thrust, BP: Brabant Para-autochthonous Unit, OTS: Overturned Thrust Sheets, OTSBT: Overturned Thrust Sheets Basal Thrust. (b) Balanced and restored cross-section of the interpreted seismic profile showing the southern Laurussian margin before the Variscan shortening event (modified from Averbuch et al., 2018). Numbers 1, 2 and 3 correspond to the order of activity of the different thrust faults.

French terminology, we will follow this classical structural nomenclature to ensure a comprehensive link with previous works in this region. From north to south, these units are the Brabant Massif, the Brabant Para-autochthonous Unit, the Overturned Thrust Sheets complex (OTS) and the Ardennes Allochthonous Unit (Belanger et al., 2012; Lacquement et al., 1999; Mansy et al., 1997; Meilliez & Mansy, 1990).

The Brabant Massif is part of the Anglo-Brabant deformation belt (Pharaoh, 2018) that was deformed during a late Caledonian orogenic event from Late Silurian to possibly Early Devonian as a result of tectonic inversion of an old Cambro-Ordovician basin (Debacker et al., 2005; Sintubin et al., 2009). It consists of a predominantly silico-clastic sedimentary sequence (sandstone, siltites, pelites) of Cambro-Silurian age, intruded by numerous deep syn-sedimentary magmatic intrusions (Legrand, 1968; Verniers et al., 2001). The lower Paleozoic substratum is unconformably overlaid to the south by a transgressive Mid-Devonian to lower Carboniferous carbonate platform sequence (Eifelian-Visean, ca. 400–330 Ma) (Bultynck et al., 1991; Mansy et al., 1999; Ziegler, 1990).

The upper Carboniferous Nord-Pas-de-Calais (NPC) coal-bearing basin overlies the Brabant lower Paleozoic basement and the Mid-Devonian to lower Carboniferous platform sequences (Figure 2). All these units constitute the foreland of the Northern Variscan thrust system. The NPC coal basin and its Devonian-lower Carboniferous substratum constitute the slightly deformed part of the Laurussian continental margin, which is classically referred to as the Brabant Para-autochthonous Unit (Figure 2a) (Hance et al., 1999; Mansy et al., 1997, 1999; Mansy & Meilliez, 1993; Meilliez & Mansy, 1990). In France, the NPC coal basin extends across 85 km E–W from the Belgian border to the Artois region and 15 km N–S from the Brabant foreland to the frontal thrust zone. Toward the east, it extends in Belgium to the Hainaut and Namur basins (Figure 1). Its stratigraphy includes an Upper Mississippian - Middle Pennsylvanian (formerly Namurian-Westphalian, ca. 320–305 Ma) synorogenic sedimentary sequence (Figure 2). Fluvio-deltaic and paralic deposits consist of a succession of alternating layers of coal, sandstones and shales, having a total thickness

19449194, 2021, 7, Downloaded from https://agupubs.onlinelibrary.wiley.com/doi/10.1029/2020TC006642 by Cochrane France, Wiley Online Library on [13/12/2023]. See the Terms and Conditions (https://onlinelibrary.wiley.com/terms-and-conditions) on Wiley Online Library for rules of use; OA articles are governed by the applicable Creative Commons License

19449194, 2021, 7, Downloaded from https://agupubs.onlinelibrary.wiley.com/doi/10.1029/2020TC006642 by Cochrane France, Wiley Online Library on [13/12/2023]. See the Terms and Conditions (https://onlinelibrary.wiley.com/terms-and-conditions) on Wiley Online Library for rules of use; OA articles are governed by the applicable Creative Commons License

of up to 3.5 kilometers (Bouroz, 1969). In the south of the study area, the upper Carboniferous sequence and its underlying substratum form a large monocline dipping gently towards the south (5–10°). It is largely underthrust below the Ardennes thrust wedge, which is generally referred to as the Ardennes Allochthonous Unit (Figure 3a). To the north, the Brabant Para-autochthonous Unit shows a clear localized flexure at the footwall of the frontal thrust zone, which allows the lower Paleozoic basement to be directly exhumed below the Cretaceous-Tertiary cover. This is the Orchies basement high located north of the NPC basin (Figure 1b). This feature has recorded the relative uplift of the Brabant foreland, that likely was coeval with the northward propagation of the thrust front (Minguely et al., 2008).

Some thrust sheets, characterized by particularly complex geometries and an overall overturned attitude of the sedimentary layers have often been observed between the Brabant Para-autochthonous Unit and the Ardennes Allochthonous Unit (Figure 3a) (Bouroz, 1969; Bouroz et al., 1961; Delmer, 1997, 2003; Lacquement et al., 1999, 2005; Mansy et al., 1997). The so-called "Overturned Thrust Sheets" are made of folded Silurian to upper Carboniferous sedimentary layers. These are frequently deformed by second-order, low-angle curved normal faults (Bouroz, 1950; Le Gall, 1994; Meilliez, 2019). The occurrence and kinematics of these faults have been observed in the coal mines (Bouroz, 1950). The OTS is a largely underconstrained body affected by a series of NNW-vergent thrust faults that hardly connect laterally. The extent of the thrust surface at the base of the OTS complex is defined here as the OTS basal thrust (OTSBT). In France, this OTS complex decreases or even vanishes west of Douai (Figure 1b).

To the south, the OTS and the Brabant Para-autochthonous Unit are overthrust by the Ardennes Allochthonous Unit along a major crustal-scale thrust fault (Figure 3a) that extends along more than 120 km to the south (Cazes et al., 1985; Mansy & Meilliez, 1993; Meilliez & Mansy, 1990; Raoult, 1986, 1988). This major thrust is named there the Allochton Main Basal Thrust (AMBT). Its shallow part is frequently referred to as the "Midi Fault" due to its recurrent position at the southern border of the coal basin ("Midi" meaning "South" in French, e.g., Meilliez, 2019). Unlike the OTS and Brabant units, the Ardennes Allochthonous Unit comprises a thick Lower Devonian sequence that was deposited in the distal rifted part of the southern Laurussian margin (Figure 2). In the Avesnois and Ardennes regions, this Lower Devonian to Dinantian sequence was intensely faulted and folded with an overall E-W to ENE-WSW strike (Khatir et al., 1988; Lacquement et al., 2005; Mansy & Lacquement, 2006; Mansy & Meilliez, 1993; Meilliez & Mansy, 1990; Moulouel, 2008). It is unconformably lying on a lower Paleozoic (Cambrian-Ordovician) slightly metamorphosed sedimentary basement that locally crops out along the frontal thrust zone. The basement crops out more substantially further south within the cores of several major thrust-related anticlinal highs such as the Rocroi, Serpont and Stavelot massifs (Figure 1b).

2.3. Current Views on the Kinematics of the Northern Variscan Front in Northern France

Restorations of geological sections and seismic profiles within the Northern Variscan thrust wedge have estimated an amount of shortening of at least 60–70 kilometers both in the Ardennes Massif (Le Gall, 1992) and at the French-Belgian border (Averbuch et al., 2018; Houchen, 1988; Lacquement, 2001; Lacquement et al., 1999; Mansy et al., 1999) (Figure 3b). A large part of the shortening is related to the major thrust zone at the base of the allochthonous unit (AMBT).

The kinematics of the AMBT has been recently documented from the interpretation and restoration of the M146 seismic profile in the Valenciennes region (Figure 3b) (Averbuch et al., 2018). The section restoration illustrates the control of the rift-related geometry of the Laurussian margin upon the Northern Variscan thrust wedge (Figure 1b and 3a). Particularly, the Devonian normal faults that formed during rifting of the Laurussian margin are likely to have localized deformation during the Variscan compression (Figure 3b) (Lacquement et al., 2005). The main border fault zone, which limits the Lower Devonian depositional area and forms a major vertical step-over in the margin geometry, is considered to have localized the main frontal ramp of the AMBT. The propagation of thrusting onto the AMBT would have induced the dissection of the crest of the related footwall block and formation of a footwall short-cut thereby inducing the transport of slices of basement and reduced Devonian-Carboniferous cover at the sole of the propagating thrust (i.e., the future OTS). The hangingwall unit (the future Ardennes Allochthonous Unit), detached on the thick basal Lower Devonian shales series, would have been displaced over the Brabant Para-autochthonous Unit forming a major thrust-related anticline, sequentially crosscut by out-of-sequence forelimb thrusts. This process

is considered to have induced the progressive shearing and overturn of the thrust-sheets involved in the initial forelimb of this major anticline. The last out-of-sequence thrust would correspond to the emergence of the AMBT along the "Midi fault zone." This propagation of thrusting along the AMBT is shown by the thrust sequence 1, 2, 3 in the restored section (Figure 3b).

The geometry and kinematics of deformation within the Northern Variscan thrust front were strongly governed by the rheological contrasts within the Paleozoic sequence. The mechanical stratigraphy within the thrust wedge is illustrated in Figure 2. As defined by structural field studies in the Ardennes-Avesnois fold-and-thrust belt (e.g., Khatir et al., 1992; Lacquement, 2001; Lacquement et al., 2005; Moulouel, 2008), three major décollements are present (Figure 2). The basal one is the weak Lochkovian shales located at the base of the syn-rift sequence. The middle one is the weak Famennian shales, resting above the more resistant Frasnian limestone unit. The upper one is located at the transition between the Dinantian carbonates and the overlying Namurian shales at the base of the synorogenic sequence. Some second-order décollements have also been described adding locally some complexity to the primary structural fold-thrust pattern. These are located within (Figure 2): (a) the shaly intervals of the Lower Devonian silicoclastic sequence; (b) the Middle Devonian shales, alternating with limestones; and (c) the numerous layers of shales of the syn-orogenic Namurian-Westphalian coal-bearing succession. It is worth noting that décollements may also exist within the carbonate-dominated Dinantian, especially in the Visean evaporitic intervals (e.g., Rouchy et al., 1986, 1987; De Putter, 1995) and in the lower part of the Tournaisian that includes shale formations, such as the homogeneous Pont d'Arcole Formation (e.g., Mortelmans and Bourguignon, 1954; Coen-Aubert et al., 1980; Poty et al., 2001; Hance and Poty, 2006).

3. Seismic and Well Data

During the 1960's and the 1980's, northern France was a target of significant onshore oil exploration by various oil and gas companies. These exploration surveys led to the acquisition of 189 seismic reflection profiles with a total length of 2,613 km. These data are essential to image the 3-D structure of the Northern Variscan Front buried under the Mesozoic-Cenozoic cover.

Our study is based on the reprocessing of 21 seismic reflection profiles acquired in the 1980's of a total length of 532 km (Figure 4). These seismic profiles were selected based on their location, their orientation, the availability and the quality of the seismic data. The selected profiles cover an approximate surface of 5,130 km^2 (95 km long by 54 km wide). They extend over the southern allochthonous and northern para-autochthonous units of the Northern Variscan Front from the cities of Arras and Lens to the west to the Belgian border to the east. They intersect the study area with various orientations, and therefore provide the opportunity to crosscut the main regional structures and to image their lateral variations. Given the acquisition parameters used in these exploration surveys, mainly the frequency bandwidth of the seismic source and the recording length (up to 5 s), the estimated depth of investigation is around 7–8 km, with a vertical resolution of approximately 25–30 meters.

Seismic reprocessing of the selected lines used modern signal-processing algorithms in order to significantly improve the quality of the images obtained in the 1980's. Efforts were focused on three key steps, repeated several times throughout the processing sequence: (a) computing primary and residual static corrections in order to remove the topographic and velocity effects of the superficial rock layer, strongly impacting the seismic signal; (b) detailed velocity analysis; and (c) various methods of organized and random noise attenuation. Pre-stack time migration enhanced the details of structural features and completed this reprocessing sequence before stacking the data.

In addition to the seismic data, three deep exploration wells have been selected and included into the database in order to provide geological information at depth along the seismic profiles. These are the Epinoy-1, Gouzeaucourt-101 and Jeumont-1 wells (Figure 4). They were selected based on their proximity to the seismic lines (less than 1 km), their depth, and the availability of well log data.

19449194, 2021, 7, Downloaded from https://agupubs.onlinelibrary.wiley.com/doi/10.1029/2020TC006642 by Cochrane France, Wiley Online Library on [13/12/2023]. See the Terms and Conditions (https://onlinelibrary.wiley.com/terms-and-conditions) on Wiley Online Library for rules of use; OA articles are governed by the applicable Creative Commons License

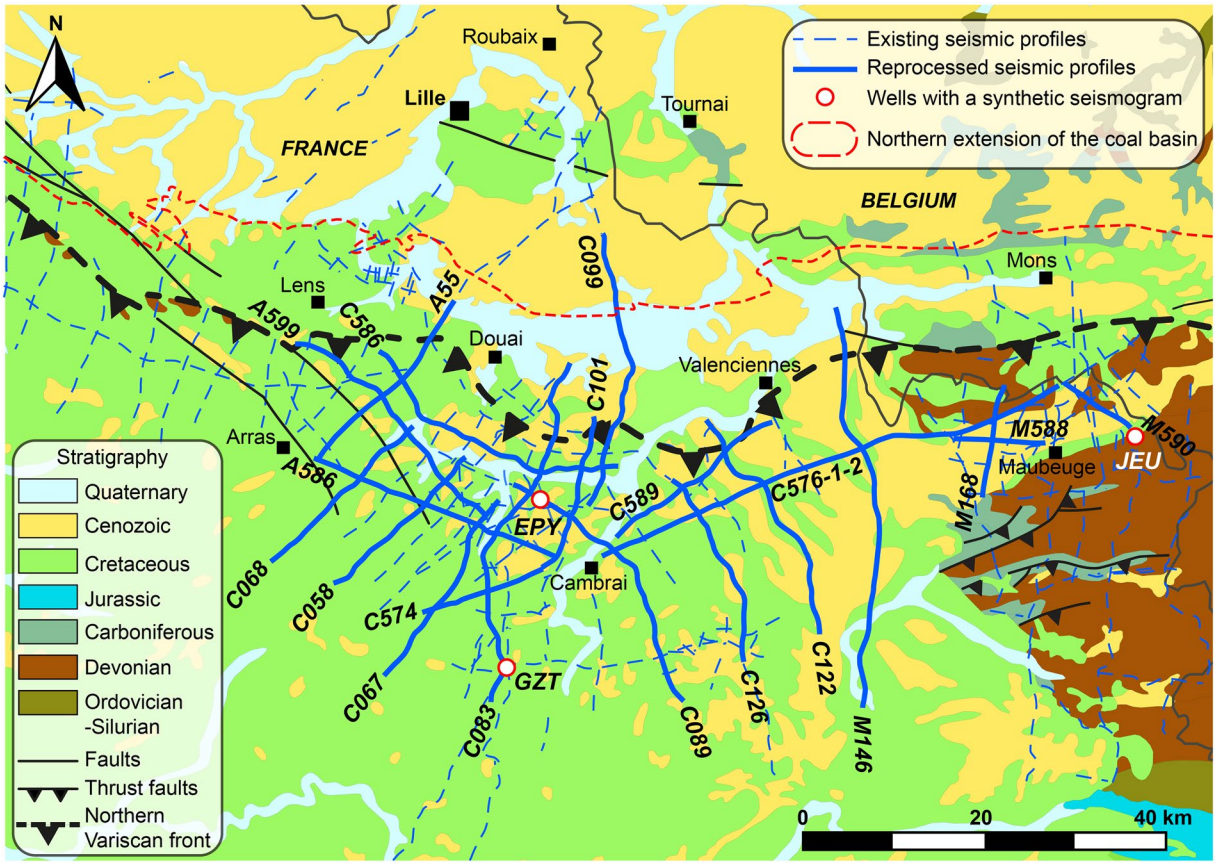

Figure 4. Simplified geological map of northern France extracted from the geological map of France (Chantraine et al., 2003) showing the location of reprocessed seismic profiles and available deep boreholes in the study area. The outline of the Northern Variscan Front corresponds to that defined before this study was conducted.

4. Seismic-Well Tie and Description of the Seismic Facies

Major stratigraphic and structural surfaces have been selected and interpreted to accurately decipher the structural framework of the thrust front. Thus, we preferentially picked the Top Paleozoic Unconformity (TPU), the AMBT, the tops of the Dinantian (T-Din), Famennian (T-Fam), Frasnian (T-Fra), Eifelian-Givetian (T-Giv) and, finally, the top of the lower Paleozoic basement (T-Sil) (Figure 5). The interpretation of the seismic data was carried out using the IHS Kingdom Software.

4.1. Seismic-Well Tie

The first step in this process was to calibrate and tie the targeted seismic markers to their corresponding geological surfaces. Two exploration wells were selected to produce synthetic seismograms: Epinoy-1 (EPY) and Jeumont-1 (JEU) (Figure 4). A synthetic seismogram is a theoretical seismic trace that models the changes in acoustic impedance in the different rock layers along a given borehole. It is generated by convolving the reflective coefficient, computed from sonic and density logs, with a seismic wavelet defining the amplitude variations of the synthetic seismogram and best representing the seismic signal.

The Epinoy and Jeumont boreholes are the only wells in the vicinity of the seismic lines that meet two important requirements: (a) the velocity data necessary for calculating a synthetic seismogram are available (sonic log, check-shots), and (b) the wells are deep enough to cross the targeted geological surfaces. Both wells drilled through the Mesozoic-Cenozoic cover, the Ardennes Allochthonous Unit and the OTS, but only the Jeumont borehole went through the entire underlying Para-autochthonous Unit and reached the

19449194, 2021, 7, Downloaded from https://agupubs.onlinelibrary.wiley.com/doi/10.1029/2020TC006642 by Cochrane France, Wiley Online Library on [13/12/2023]. See the Terms and Conditions (https://onlinelibrary.wiley.com/terms-and-conditions) on Wiley Online Library for rules of use; OA articles are governed by the applicable Creative Commons License

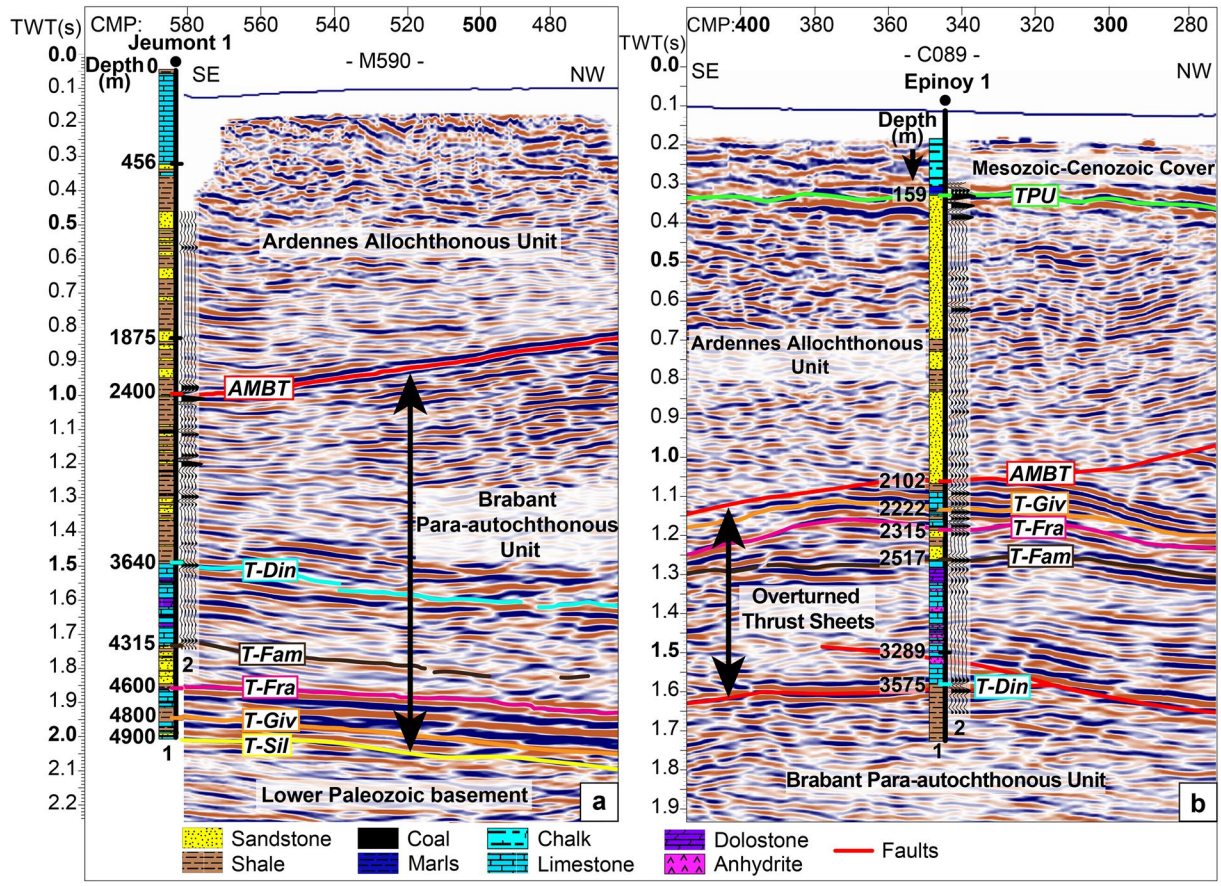

Figure 5. Seismic-well tie between (a) the Jeumont borehole and the M590 reprocessed seismic profile, and (b) the Epinoy borehole and the C089 reprocessed seismic profile. 1: Lithological log; 2: Synthetic seismogram. T-Din: Top Dinantian; T-Fam: Top Famennian; T-Fra: Top Frasnian; T-Giv: Top Givetian; T-Sil: Top Silurian; TPU: Top Paleozoic Unconformity.

Eifelian (Figure 5). Therefore, the Epinoy and Jeumont boreholes have been used as references to identify the seismic markers in the OTS and in the Para-autochthonous Unit.

Synthetic seismograms were generated following several steps: (a) quality control of the sonic log and removal of abnormal values; (b) integration of the velocity data (sonic log and check-shots); (c) generation of a time-depth chart that allowed us to convert the vertical scale of the well data from depth to time using integrated velocity data; (d) setting the density value to 1 g/cm^3, as the density logs were not available; (e) computation of the acoustic impedance; (f) computation of the reflectivity coefficient; (g) generation of a seismic wavelet extracted from the seismic traces around the well and having a mean frequency of 35 Hz; (h) convolution of the reflectivity coefficient with a seismic wavelet. Once the synthetic seismograms were created for both wells, they were adjusted on the seismic profiles M590 (Jeumont) and C089 (Epinoy) so that they fit the seismic signal around the well, concluding the seismic-well tie process (Figure 5). The latter made it possible to calibrate and tie the geological surfaces of interest to the corresponding seismic markers, with the exception of the top of the Brabant basement that was never encountered in the boreholes.

Once the targeted horizons were identified near the Epinoy and Jeumont boreholes, they were correlated step by step from line to line by comparing the seismic facies and by checking the 3-D structural consistency. Structural surfaces, such as major thrust faults and normal faults were also interpreted and correlated from line to line. These faults usually appeared as discontinuities delimiting and truncating two sets of reflectors often having a different apparent dip. This sparse well data set could be seen as a source of interpretation uncertainties; this is however compensated by the lateral coherence of the seismic facies and structures throughout the study area, thereby helping the seismic interpretation process.

19449194, 2021, 7, Downloaded from https://agupubs.onlinelibrary.wiley.com/doi/10.1029/2020TC006642 by Cochrane France, Wiley Online Library on [13/12/2023]. See the Terms and Conditions (https://onlinelibrary.wiley.com/terms-and-conditions) on Wiley Online Library for rules of use; OA articles are governed by the applicable Creative Commons License

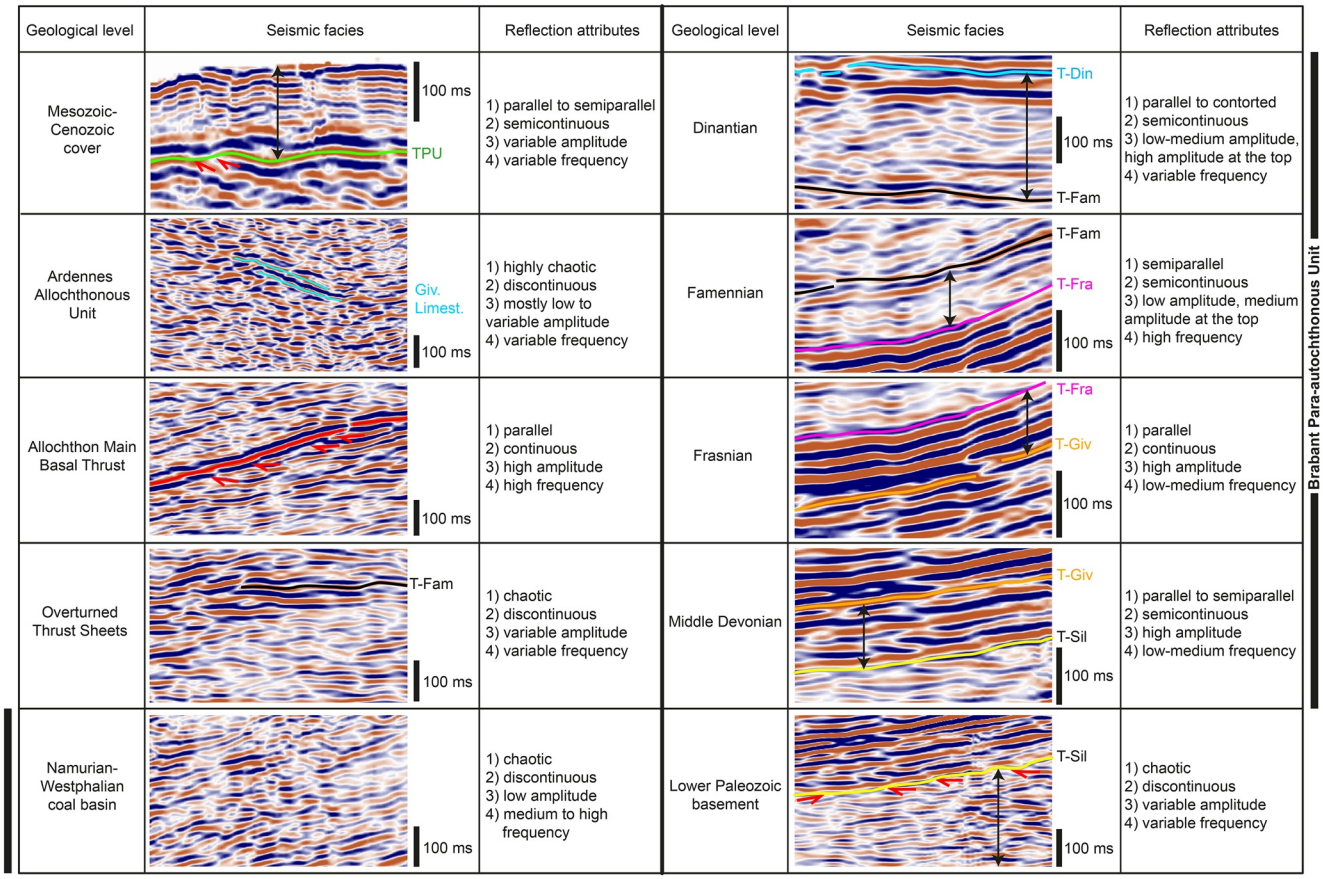

Figure 6. Illustration and description of the characteristic seismic facies of the interpreted geological formations and units. Reflection attributes: a) configuration; b) continuity; c) amplitude; d) frequency. Giv. Limest.: Givetian limestones; T-Din: Top Dinantian; T-Fam: Top Famennian; T-Fra: Top Frasnian; T-Giv: Top Givetian; T-Sil: Top Silurian; TPU: Top Paleozoic Unconformity.

4.2. Seismic Facies

Seismic-well tie allowed to identify the targeted geological surfaces and to identify the overall seismic facies of the relevant geological units. They are described here and illustrated in Figure 6.

The Mesozoic-Cenozoic cover is represented by rather parallel to semiparallel reflectors, continuous, with high amplitude and low frequency in the lower part; in the upper part the reflectors are more or less continuous and display variable amplitude with high frequency (Figure 6). Due to the unconformable character of the Mesozoic-Cenozoic cover on the Paleozoic substratum, the Top Paleozoic Unconformity is usually identified by truncations below parallel, continuous and high amplitude reflectors (Figure 6).

The Ardennes Allochthonous Unit is located beneath the Mesozoic-Cenozoic sedimentary cover. It is characterized by an overall chaotic seismic sequence with discontinuous reflectors having variable amplitude and frequency (Figure 6). The intense deformation of the allochthonous series, which are affected by numerous faults and sometimes very steep or even vertical or overturned folds, generates strong dispersions of the seismic waves. This makes it difficult to obtain a good seismic imaging of this unit. However, some continuous, high-amplitude reflectors sporadically and locally appear on a few profiles (Figure 6). These have been interpreted as the Givetian limestones (Lacquement et al., 1999).

The AMBT, which is located at the base of the Allochthonous Unit, is usually clearly visible on the seismic profiles. It is represented by a series of few continuous and parallel reflectors of high amplitude and frequency, truncating locally reflectors at its footwall (the underlying OTS and Brabant Para-autochthonous Unit) (e.g., Raoult, 1986; Lacquement et al., 1999) (Figure 6).

19449194, 2021, 7, Downloaded from https://agupubs.onlinelibrary.wiley.com/doi/10.1029/2020TC006642 by Cochrane France, Wiley Online Library on [13/12/2023]. See the Terms and Conditions (https://onlinelibrary.wiley.com/terms-and-conditions) on Wiley Online Library for rules of use; OA articles are governed by the applicable Creative Commons License

Below the AMBT, the OTS are distinguished by rather chaotic facies associated with discontinuous reflectors of variable amplitude and frequency (Figure 6). The intense deformation of the OTS makes it difficult to image their internal geometry. However, continuous reflectors are visible in some areas (see Figure 5b). The OTSBT is not always easily visible on the profiles; its seismic facies vary laterally, depending on the impedance contrast between the footwall and hangingwall formations. In areas where there is a strong impedance contrast, for instance between Dinantian carbonates in the OTS and Namurian shales in the para-autochthonous unit, the OTSBT is represented by a series of parallel and rather continuous high amplitude reflectors. On the contrary, the weak impedance contrast created by the presence of Namurian deposits both in the hangingwall and footwall of the OTSBT results in a lower amplitude seismic facies of the OTSBT.

The Brabant Parautochtonous Unit is characterized by variable seismic facies: (a) the Namurian-Westphalian coal-bearing deposits are characterized by a chaotic seismic facies. The reflectors are discontinuous and usually have a low amplitude and a medium-to-high frequency (Figure 6). These chaotic facies can be related to the intense short-wavelength folding and faulting of the coal basin during the late Carboniferous, which is responsible for the strong dispersion of the seismic waves; (b) the underlying Dinantian carbonate platform is represented by a parallel to contorted facies, associated with semicontinuous reflectors of variable frequency and medium-to-low amplitude (Figure 6). In some areas, the Dinantian displays semi-transparent seismic facies associated with very low-amplitude reflections. At the top of the Dinantian, the reflectors are usually continuous and have a higher amplitude (Figure 6), illustrating a major impedance variation between the overlying Namurian coal-bearing deposits and the Visean limestones; (c) Famennian sedimentary sequences, comprising mainly sandstones and shales, appear as semiparallel, semicontinuous, low-amplitude and high-frequency reflectors (Figure 6). The top of Famennian is usually visible on seismic lines because it appears as continuous medium-amplitude and high-frequency reflectors (Figure 6); (d) beneath the Famennian, the Frasnian limestones are marked by their stratified geometry associated with parallel, continuous, high-amplitude and low-frequency reflectors, easily visible on seismic data (e.g., Raoult, 1986; Lacquement et al., 1999) (Figure 6); (e) the underlying Eifelian-Givetian limestones have a similar seismic facies, although the reflectors are mostly semicontinuous (Figure 6).

At the base of the Brabant Para-autochthonous Unit, the Eifelian and Givetian limestones are unconformably lying above Silurian deposits of the lower Paleozoic basement. The latter is represented by a chaotic facies associated with discontinuous reflectors of variable amplitude and frequency (Figure 6). Poor imaging of the basement structure is due to the low penetration of seismic waves at such depths. The basement unconformity is poorly imaged on seismic lines. It can usually be identified as the limit between the chaotic facies of the basement and the semicontinuous high-amplitude reflectors of the Eifelian-Givetian limestones. Truncations of the basement reflectors below the Middle Devonian deposits are sometimes visible (Figure 6).

5. Seismic Interpretation

The interpretation of the seismic lines provides insights into the geometric and structural features of the Northern Variscan Front and its substratum. We were able to evidence the first-order geometry of major extensional and compressional structures and present it below. The description follows the structural model described above (cf., 2.2.), detailing the geometry of the Brabant Para-autochthonous Unit, the Overturned Thrust Sheet and the Ardennes Allochthonous Unit. In particular, we focus on lateral ramps within the thrust system.

5.1. Brabant Para-Autochthonous Unit

The relatively good quality of seismic data below the poorly imaged Ardennes Allochthonous Unit allows us to precisely interpret the deep structure of the buried Brabant Para-autochthonous Unit. In the following, we successively document the large underthrusting of the foreland basin below the AMBT, second order thrust faults, deep folding and then extensional structures in the Brabant Para-autochthonous Unit.

19449194, 2021, 7, Downloaded from https://agupubs.onlinelibrary.wiley.com/doi/10.1029/2020TC006642 by Cochrane France, Wiley Online Library on [13/12/2023]. See the Terms and Conditions (https://onlinelibrary.wiley.com/terms-and-conditions) on Wiley Online Library for rules of use; OA articles are governed by the applicable Creative Commons License

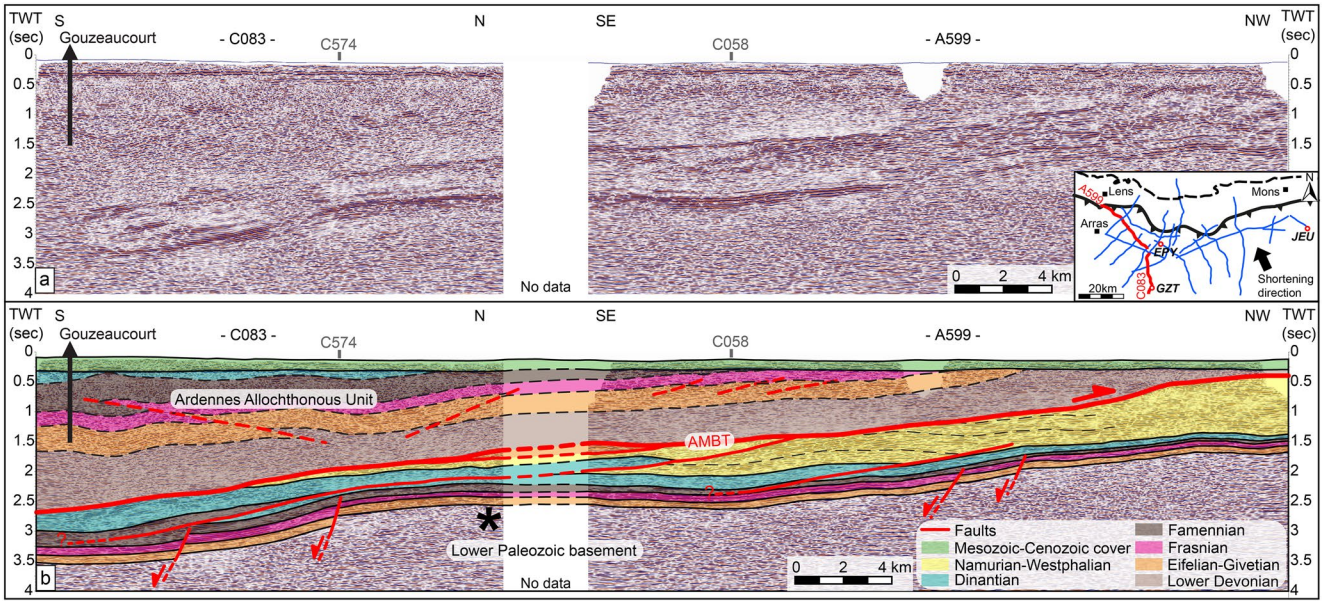

Figure 7. SE-NW composite seismic reflection profile with (a) reprocessed line and (b) geological interpretation. This profile is approximately parallel to the Variscan shortening direction (i.e., SE-NW). The dashed lines in the Namurian-Westphalian coal basin represent the overall geometry of the sedimentary layers. The asterisk marks the deep low-curvature folding of the Brabant Para-autochthonous Unit.

5.1.1. Extent of Foreland Basin Underthrusting

Seismic interpretation of profiles oriented parallel to the overall thrust transport direction (NNW-SSE) such as the A599-C083 composite seismic profile (Figure 7), highlights the large underthrusting of the Brabant Parautochthonous Unit below the Ardennes Allochthonous Unit. Identifying the cut-off line of the basal reflector of the Namurian–Westphalian foreland basin with the AMBT allowed us to quantify the relative minimum amount of underthrusting of the foreland basin beneath the allochthonous unit. It reveals that the sub-thrust foreland basin extends c. 20–25 km beyond the thrust front. More than half of the coal-basin region is therefore buried below the AMBT. This pattern observed on all seismic profiles in the study area (e.g., C122 profile in Figure 8) underlines highly localized displacement onto the AMBT and its subsidiary, the OTSBT.

5.1.2. Second-Order Variscan Thrust Faults

The interpretation of the C122 profile, trending parallel to the direction of the Variscan shortening, shows two major NW-verging thrust faults that deform the Brabant Para-autochthonous Unit below the AMBT (Figure 8). Truncations of the reflectors are clearly visible against the footwall of these faults. The upper thrust is truncated to the south by the AMBT and deforms the Namurian-Westphalian coal-bearing deposits. The lower thrust affects the coal basin, as well as the underlying Dinantian and Famennian platforms. Both thrusts show two flats and ramps. The geometry of the reflectors on the hangingwall of these faults indicates a major folding of the Brabant para-autochthonous sequence, especially in the coal basin. We interpreted those folds as fault-bend folds generated by the movement of the thrust sheets over the ramps (e.g., Suppe, 1983). Accordingly, these two thrusts formed along two of the main regional detachments: the upper one located at the limit between the Dinantian carbonates and the Namurian shales and sandstones and the lower one located within the Famennian shales, resting onto the Frasnian limestones (Figure 2). These compressional structures have been interpreted on numerous seismic profiles and are consistent in the entire study area.

The interpretation of the C058 profile (Figure 9), oriented almost perpendicularly to the regional thrust transport direction, provides another example of a deep thrust characterized by a detachment in the Famennian shales. This thrust has an apparent dip towards the SW and affects the Famennian to Namurian-Westphalian sequence.

19449194, 2021, 7, Downloaded from https://agupubs.onlinelibrary.wiley.com/doi/10.1029/2020TC006642 by Cochrane France, Wiley Online Library on [13/12/2023]. See the Terms and Conditions (https://onlinelibrary.wiley.com/terms-and-conditions) on Wiley Online Library for rules of use; OA articles are governed by the applicable Creative Commons License

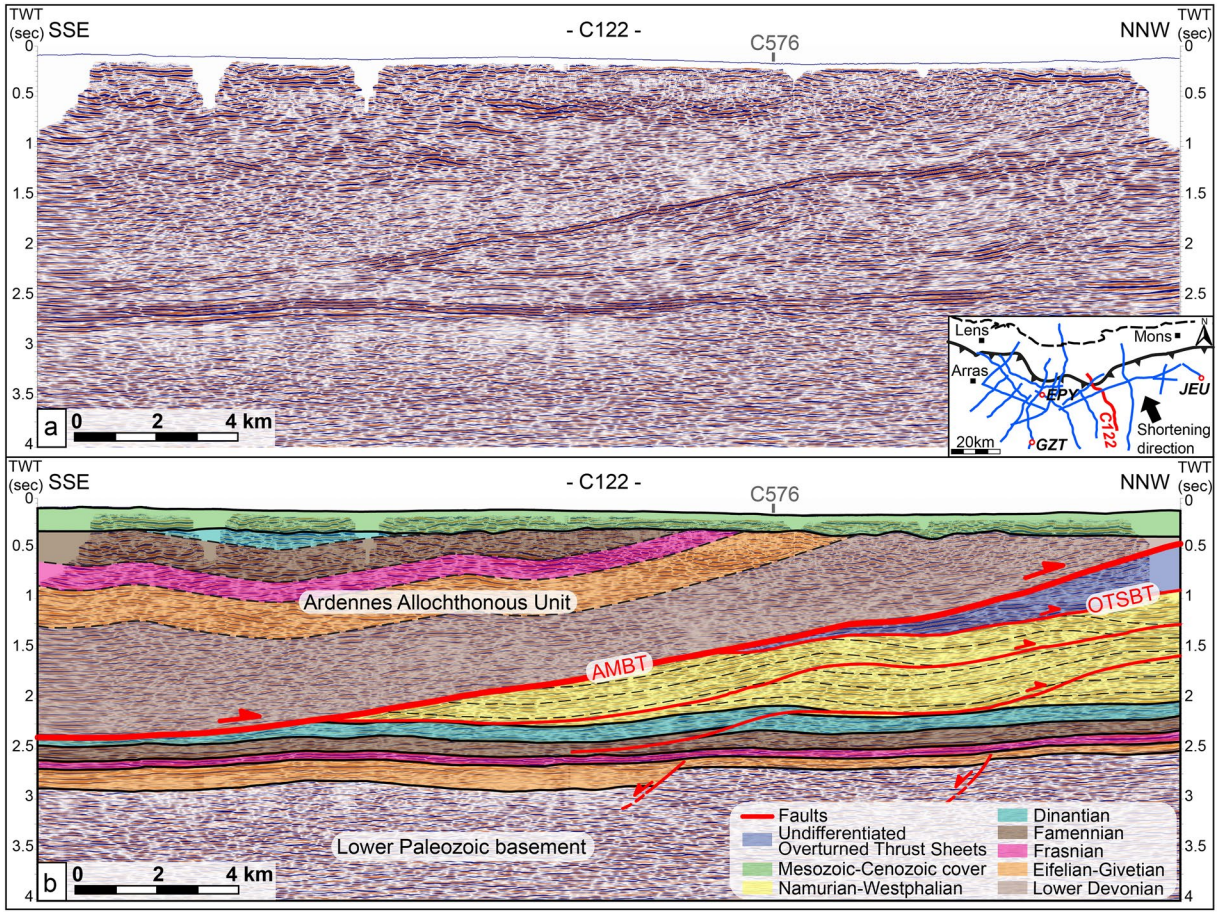

Figure 8. Seismic reflection profile C122 (in TWT) with (a) reprocessed line and (b) geological interpretation. This profile is almost parallel to the Variscan shortening direction (i.e., SE-NW). The dashed lines in the Namurian-Westphalian coal basin represent the overall geometry of the sedimentary layers. The dashed lines in the Ardennes Allochthonous Unit emphasize the simplified nature of the interpretation and the related uncertainties.

A similar geometry has also been observed on the C083 profile (Figure 10). A major thrust is visible on the entire profile and characterized by an apparent southward dip. It deforms the Famennian to Westphalian para-autochthonous sequence and is responsible for its northward displacement of at least 4 km. Truncations of the reflectors, both against the footwall and the hangingwall of this fault, allowed us to delineate its geometry made of one flat and two ramps. Deformation was rooted into the Famennian detachment at the southern end of the profile. The existence of a flat within the generally competent Dinantian carbonates is quite surprising, but its occurrence appeared reasonable in 3-D. The involved décollement in the Dinantian could correspond to the Visean evaporites or the shaly formations of the Tournaisian (e.g., Pont d'Arcole Formation) (Figure 2).

Thrust faults rooting within the Famennian shales and deforming the Famennian to upper Carboniferous series are visible on most seismic lines. Their generalized character along the Northern Variscan Front is particularly well illustrated on a WSW-ENE composite seismic profile (Figure 11) that crosses the entire study area. Since the composite profile is almost orthogonal with respect to the Variscan shortening direction (i.e., SE-NW), it is important to notice that structures are intersected at a high angle relative to the main plane of movement. Six of these highlighted thrusts have an apparent vergence towards the WSW and an apparent dip towards the ENE. The folded geometry of the reflectors in the hangingwall of some of these faults indicates the existence of thrust-related folds generated by movement of the thrust sheets over the ramps. A peculiar feature to note on this profile (Figure 11) is the existence of a thrust fault rooting down onto the Middle Devonian second-order décollement (Figure 2). It is also important to notice that this fault apparently nucleated against a Middle Devonian normal fault.

19449194, 2021, 7, Downloaded from https://agupubs.onlinelibrary.wiley.com/doi/10.1029/2020TC006642 by Cochrane France, Wiley Online Library on [13/12/2023]. See the Terms and Conditions (https://onlinelibrary.wiley.com/terms-and-conditions) on Wiley Online Library for rules of use; OA articles are governed by the applicable Creative Commons License

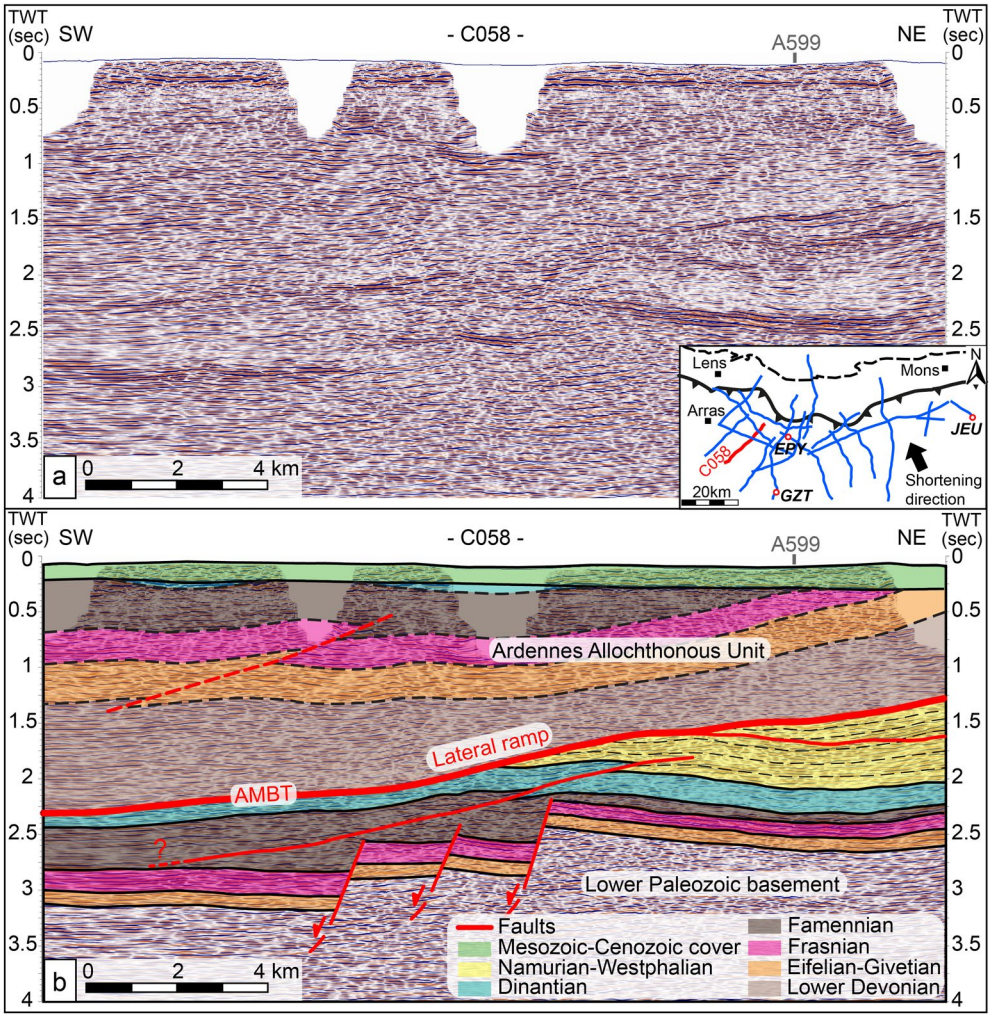

Figure 9. Seismic reflection profile C058 with (a) reprocessed line and (b) geological interpretation. This profile is highly oblique with respect to the direction of Variscan shortening (i.e., SE-NW). The dashed lines in the Namurian-Westphalian coal basin represent the overall geometry of the sedimentary layers. The dashed lines in the Ardennes Allochthonous Unit mark the simplified geometry of the interpretation and the related uncertainties.

5.1.3. Deep Folding of the Para-Autochthnous Unit

The interpretation of the C083 profile (Figure 10) illustrates the overall southward dip of the Brabant Para-autochthonous Unit, as well as some superimposed long-wavelength ondulations of the basement and the overlying para-autochthonous series. A gentle antiform structure is observed west of Cambrai in the southern part of the profile (marked by an asterisk in Figure 10) at a depth over 2 s TWT. This long-wavelength, deep antiform affects the lower Paleozoic basement and the entire para-autochthonous sequence. Similar deep folding of the basement and the Brabant Para-autochthonous Unit has also been observed further west on the C058, C067 and C068 profiles. For instance, on the C058 profile (Figure 9), Devonian and Carboniferous layers at the footwall of the northernmost Devonian normal fault are dipping northward.

We do not view this peculiar geometry as a seismic artifact (pull-up effect) because there is no evidence of the presence of a high seismic velocity layer above the para-autochthonous unit. Seismic facies of the Ardennes Allochthonous Unit remain consistent across the profiles (Figure 10). Moreover, the AMBT does not seem to be affected by this uplift as it would be the case with a seismic pull up. Instead, we suggest that this basement dome corresponds to a deep anticline formed during the propagation of the Variscan thrust front. The lack of deformation of the AMBT, which truncates the folded para-autochthonous series

19449194, 2021, 7, Downloaded from https://agupubs.onlinelibrary.wiley.com/doi/10.1029/2020TC006642 by Cochrane France, Wiley Online Library on [13/12/2023]. See the Terms and Conditions (https://onlinelibrary.wiley.com/terms-and-conditions) on Wiley Online Library for rules of use; OA articles are governed by the applicable Creative Commons License

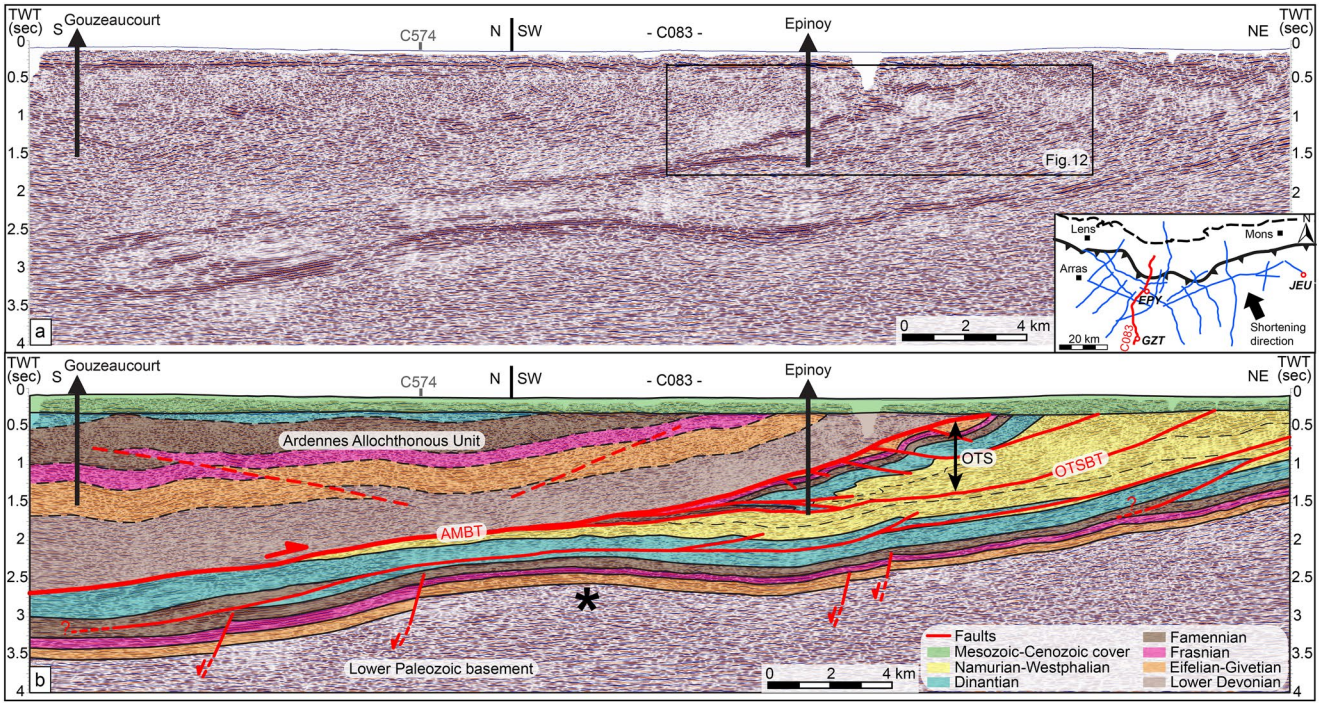

Figure 10. Seismic reflection profile C083 with (a) reprocessed line and (b) geological interpretation. This profile is mostly parallel to the Variscan shortening direction (i.e., SE-NW) in its southern part and highly oblique to the Variscan shortening direction in its northern part. The asterisk points out folding at depth of the Brabant para-autochthonous Unit. The black frame corresponds to an enlarged part of this profile focusing on the OTS internal structure, presented in Figure 12.

(Figure 10), suggests that the anticline formed before the terminal stage of the Variscan orogeny and the out-of-sequence dislocation of the frontal thrust zone in the Middle Pennsylvanian (i.e., late Westphalian).

5.1.4. Pre-Existing Extensional Structures

The clearly imaged deep reflectors below the AMBT provide useful insights on the prominent characteristics of the initial geometry of the Laurussian margin prior to its underthrusting. For example, this is illustrated by the C122 profile located south of Valenciennes (Figure 8). Analysis of the reflectors' continuity and the seismic facies variation shows two normal faults with an apparent southward dip. These faults affect the lower Paleozoic basement and offset the top of the basement. The southernmost normal fault is particularly well marked by the contrasting seismic facies of the Middle Devonian in its hangingwall (i.e., rather transparent facies) and footwall (i.e., higher amplitude reflectors). The Eifelian-Givetian deposits are thicker in the hangingwall of these faults, thus demonstrating the syn-sedimentary nature of these extensional structures (i.e., Middle Devonian in age). The continuity of the high amplitude reflectors of the Frasnian limestones above those faults suggests that deformation ended before the Late Devonian. Similar faults have been interpreted in the eastern part of the study area, especially on the M146 profile (Figure 3) (Lacquement et al., 1999).

Further west, south of Douai, our interpretation of the seismic lines C058 (Figure 9), C067, C068 and C083 (Figure 10) highlights a series of normal faults that have apparent dips towards the south or southwest. Large offsets of high-amplitude, usually continuous, reflectors of the Frasnian limestones are clearly visible on these profiles, especially the C058 one (Figure 9). The analysis of these offsets allowed to identify two to three major normal faults in the southern part of the profiles. These faults clearly deform the basement and the Middle Devonian sediments. Thickening of the Frasnian and mostly of the Famennian, is visible in their hangingwall, evidencing the apparent syn-sedimentary nature of these extensional structures (i.e., Late Devonian in age). Along the C058 (Figure 9) and C083 profiles (Figure 10), Devonian normal faults are particularly well imaged because the strike of the profiles (i.e., SW-NE) is orthogonal to the strike of the normal faults (i.e., NW-SE–see later in 6.3.).

19449194, 2021, 7, Downloaded from https://agupubs.onlinelibrary.wiley.com/doi/10.1029/2020TC006642 by Cochrane France, Wiley Online Library on [13/12/2023]. See the Terms and Conditions (https://onlinelibrary.wiley.com/terms-and-conditions) on Wiley Online Library for rules of use; OA articles are governed by the applicable Creative Commons License

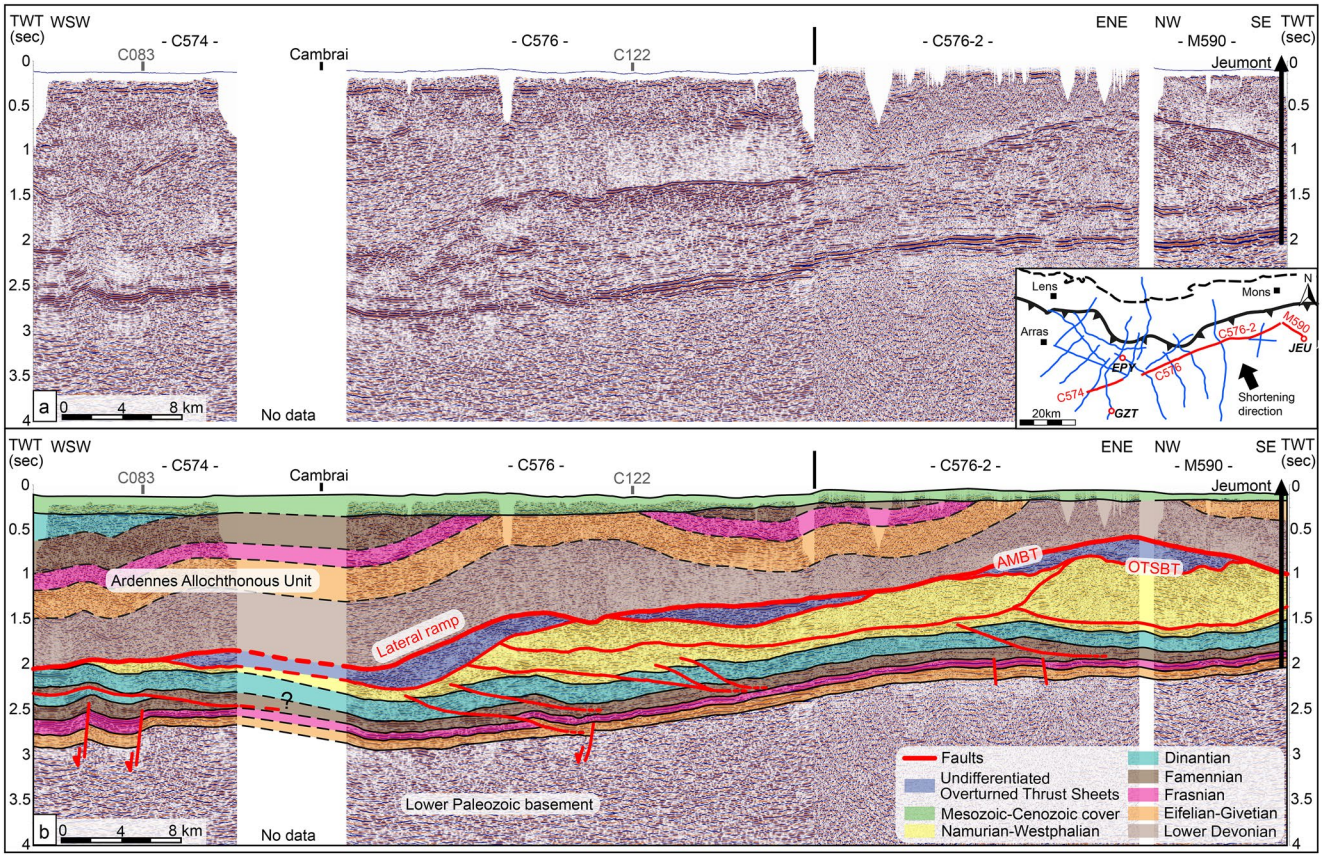

Figure 11. WSW-ENE composite seismic reflection profile with (a) reprocessed line and (b) geological interpretation. Note that the strike of this profile is orthogonal to the Variscan shortening direction (i.e., SE-NW), implying that structures are intersected very obliquely with respect to the direction of tectonic movement.

In summary, deep Devonian syn-sedimentary normal faults are visible on most of the interpreted profiles. These faults accommodated extension during the Mid-Late Devonian and represent first-order structures of the pre-orogenic Laurussian margin in its proximal part (Brabant border). These results suggest that extensional deformation persisted after the Early Devonian rifting phase associated with the opening of the Rheno-Hercynian Ocean and responsible for the first-order segmentation of the southern Laurussian margin. This post-rift extension, coeval with the overall thermal subsidence of the margin, may have had some impacts on its structure and the associated depocenters until the Famennian, at least in the most proximal part of the margin (the southern border of the Brabant massif). This result is in agreement with several studies carried out along the Northern Variscan Front (Ardennes, southern England) that evidenced some effects of extension on the sedimentation pattern up to the Middle and Late Devonian (e.g., Thorez & Dreesen, 1986; Préat & Boulvain, 1988; Shail & Leveridge, 2009; Leveridge, 2011). Interestingly, an analysis of the faults' activity shows a diachronic pattern within the study area. Some faults were active during the Middle Devonian and others during the Late Devonian. The reason for such diachronism in northern France remains an open question. Similar diachronic segmentation of the Laurussian margin is also known in SW England where a progressive northward development of the Laurussian margin basins between the Emsian (Looe Basin) and the Famennian (Culm basin) has been highlighted (Leveridge, 2011; Shail & Leveridge, 2009).

Finally, comparison of the position of Devonian syn-sedimentary normal faults and Variscan thrust faults indicates that most ramps of the Variscan thrusts (both lateral and frontal) are located above Middle to Late Devonian syn-sedimentary normal faults. For instance, the ramps of both thrusts in the Para-autochthonous Unit on the C122 profile (Figure 8) are located above two Middle Devonian normal faults. Moreover, the lower detachment within the Famennian is located right above the southern normal fault. The same observation has been made on the C058 profile (Figure 9), where the lateral ramp of the AMBT and the

19449194, 2021, 7, Downloaded from https://agupubs.onlinelibrary.wiley.com/doi/10.1029/2020TC006642 by Cochrane France, Wiley Online Library on [13/12/2023]. See the Terms and Conditions (https://onlinelibrary.wiley.com/terms-and-conditions) on Wiley Online Library for rules of use; OA articles are governed by the applicable Creative Commons License

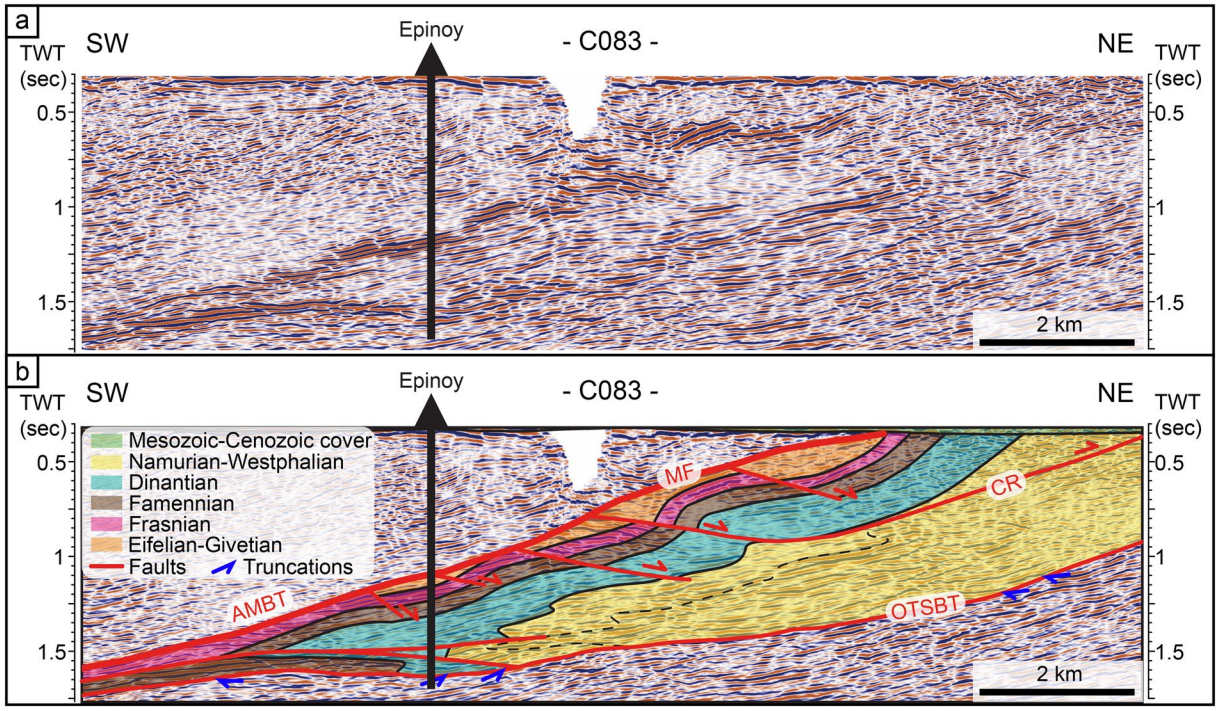

Figure 12. Details on the internal structure of the OTS on the seismic reflection profile C083; (a) reprocessed line and (b) geological interpretation. This part of the profile is oblique to the Variscan shortening direction (i.e., SE-NW). The structures are intersected obliquely with respect to the tectonic transport direction. Faults legend: CR: "Cran de Retour"; MF: "Midi Fault".

ramp of the para-autochthonous thrust are located above a series of three Late Devonian syn-sedimentary normal faults. The same feature can be observed on the C083 profile (Figure 10) where both ramps of the major thrust fault in the Para-autochthonous Unit are located above Devonian normal faults.

5.2. Overturned Thrust Sheets

The OTS constitute one of the major and peculiar units of the Northern Variscan Front in the north of France. Owing to the seismic-well tie of the Epinoy borehole, we could link the overall and internal structure of the OTS between Douai and Cambrai cities (Figure 10 and 12). The OTS are bounded by two major thrusts characterized by high amplitude seismic facies. These are the out-of-sequence "Midi Fault" at the top, which corresponds to the shallower part of the AMBT, and the OTSBT that connects to the AMBT south of the profile.

The internal structure of the OTS (Figure 12) is interpreted on the basis of (a) the stratigraphic succession known from the Epinoy borehole, (b) the geometry of the reflectors, (c) the 3-D consistency with structures interpreted on all related seismic profiles, and (d) the consistency with the near surface structures in the coal basin area (Bouroz et al., 1963) (Figure 12). The interpretation of the C083 seismic line shows the overturned geometry of the Devonian-Carboniferous sequence that is deformed as a major recumbent syncline. It is worth mentioning that imaging of a recumbent fold in seismic data is limited, particularly in the hinge zone, where reflectors of both the upper and lower limbs intersect, creating mostly chaotic and discontinuous seismic patterns. Therefore, some uncertainties remain on the position of markers interpreted in the hinge zone of recumbent synclines, where interpretation choices have to be made to maintain a coherent geometry and kinematics.

The north-facing recumbent syncline is truncated to the south by the AMBT. It is characterized by a significant thickening of the sedimentary series across the hinge zone. This is especially the case for the Dinantian sequence observed in the Epinoy borehole whose thickness reaches at least a thousand meters. The overturned limb of the syncline is deformed by northward-dipping second-order low-angle curved normal faults

19449194, 2021, 7, Downloaded from https://agupubs.onlinelibrary.wiley.com/doi/10.1029/2020TC006642 by Cochrane France, Wiley Online Library on [13/12/2023]. See the Terms and Conditions (https://onlinelibrary.wiley.com/terms-and-conditions) on Wiley Online Library for rules of use; OA articles are governed by the applicable Creative Commons License

present in the coal basin (Bouroz, 1950; Le Gall, 1994; Meilliez, 2019). It is also truncated by a NE-verging thrust fault bounded to the south by the AMBT. This curved thrust has been identified as the "Cran de Retour" thrust (CR), described in the NPC coal basin literature (e.g., Bouroz et al., 1961; Becq-Giraudon, 1983).

5.3. Ardennes Allochthonous Unit

The Ardennes Allochthonous Unit is not well imaged on seismic data, mainly because of the combined effect of an overall lithological homogeneity of the sedimentary sequences (mostly alternating shales and sandstones) and intense internal deformation. Despite this, our interpretation is based on (a) the seismic-well tie of the Gouzeaucourt borehole (GZT) along with the C083 profile (Figure 10), (b) the interpretation of some sporadic and continuous high-amplitude reflectors that we assume to correspond to Givetian limestones (Lacquement et al., 1999; Raoult, 1986), (c) the geological sketch map of the Paleozoic substratum in northern France (C.F.P. et al., 1965; Figure 1b), (d) the 3-D coherence between profiles.

Our interpretations are greatly simplified compared with the present-day structure of the Allochthonous Unit, but they highlight locally some major Variscan folds and thrusts affecting the Lower Devonian to lower Carboniferous allochthonous sequence. For instance, a north-vergent thrust fault deforming the Lower to Upper Devonian layers has been interpreted on the C058 (Figure 9) and C083 (Figure 10) profiles. A back-thrust can also be seen on the C083 profile (Figure 10). It is characterized by a detachment in the Lower Devonian series (Figure 2) and it deforms the entire Devonian allochthonous sequence. Such back-thrusts in the Ardennes Allochthonous Unit have already been observed and described in the field in the Avesnois region (Moulouel, 2008).

5.4. Lateral Ramps in the Thrust System

In the area SE of Douai, near Cambrai, specific structural features along the AMBT are present and are illustrated on the composite WSW-ENE striking seismic line (Figure 11). In the eastern part of the C576 profile, the AMBT trace is mostly parallel to the surface and is only slightly tilted toward the south at a depth of approximately 1.2–1.5 s TWT. It then rapidly deepens westward at a depth of 2 s TWT. This phenomenon is associated with significant folding and thickening of the overlying Ardennes Allochthonous Unit. Considering that the orientation of this seismic profile is orthogonal to the direction of the Variscan shortening, we interpreted this change in geometry of the thrust fault as an evidence of a major lateral or oblique ramp in the western part of the profile. Lateral and oblique ramps are defined as thrust surfaces that are parallel or oblique to the direction of transport of the allochthonous thrust sheet (e.g., Butler, 1982; McClay, 1992). These have been observed and described in numerous fold-and-thrust belts, such as the Pyrenees (Averbuch et al., 1993; Frizon de Lamotte et al., 1995), Taiwan (Lacombe et al., 2003) or the Appalachians (Cook & Thomas, 2009).

The AMBT is characterized by a frontal ramp in the eastern part of the profile (south of Valenciennes). A similar example of a lateral or oblique ramp of the AMBT is visible to the west on the C058 profile that is oblique to the direction of Variscan shortening (Figure 9). Interestingly, on the C576 profile, the OTSBT has a similar lateral or oblique ramp geometry under the lateral ramp of the AMBT (Figure 11). This suggests that both thrusts may have been inherited from a similar 3-D geometry.

Finally, the underlying Para-autochthonous Unit shows a complex structure under those two superimposed lateral ramps (Figure 11). Indeed, the Middle-Upper Devonian and Carboniferous sequence is deformed by deep Variscan thrusts that have an apparent vergence towards the WSW and are associated with fault-related folds. These structures caused an overthickening of the Para-autochthonous Unit under the lateral ramps.

6. Structural Maps

Results of the seismic interpretation have been correlated and summarized on time structural maps (or isochron maps) for the key geological surfaces such as the AMBT, the OTSBT or the top of the Givetian sedimentary layer in the Brabant Para-autochthonous Unit. Structural surfaces were generated in two-way travel time (TWT time) using a minimum curvature algorithm, meaning that seismic data were interpolated

19449194, 2021, 7, Downloaded from https://agupubs.onlinelibrary.wiley.com/doi/10.1029/2020TC006642 by Cochrane France, Wiley Online Library on [13/12/2023]. See the Terms and Conditions (https://onlinelibrary.wiley.com/terms-and-conditions) on Wiley Online Library for rules of use; OA articles are governed by the applicable Creative Commons License

19449194, 2021, 7, Downloaded from https://agupubs.onlinelibrary.wiley.com/doi/10.1029/2020TC006642 by Cochrane France, Wiley Online Library on [13/12/2023]. See the Terms and Conditions (https://onlinelibrary.wiley.com/terms-and-conditions) on Wiley Online Library for rules of use; OA articles are governed by the applicable Creative Commons License

and extrapolated in 3-D based on the principle that two adjacent data points were assumed to lie along a circular arc. A medium smoothing was applied during the gridding process in order to improve the plotting quality of the isochrons while respecting the seismic data interpretation. A different grid cell size has been chosen to model the different structural horizons, depending on precision needed and structural complexity of the geological surface. For instance, we chose a 1500 × 1500 meters grid cell size to model the AMBT surface because this surface is quite homogeneous in 3-D. On contrary, we chose a 100 × 100 meters grid cell size to model the top Givetian horizon, which is much more deformed. It is important to mention a limitation associated with this modeling method. Indeed, since it is based on the interpolation of the seismic data interpretation, uncertainties increase in areas where seismic lines are located far from each other. Therefore, the results of gridding have to be considered with caution in areas with no closeby-located seismic data.

The structural maps obtained provide unprecedented regional images of the 3-D geometry of the Northern Variscan Front and the structure of the underthrust southern Laurussian margin in northern France. Furthermore, mapping of the cut-off lines of the base of the Namurian-Westphalian molasse (Figure 13a) and of the OTSBT (Figure 13b) allows to characterize the southern extent of the syn-orogenic deposits and the OTS complex below the Ardennes Allochthonous Unit. They also allow us to quantify the relative displacement on the AMBT and the related underthrusting of the Brabant Para-autochthonous Unit.

6.1. 3-D Geometry of the AMBT

The structural map of the AMBT between Arras and Maubeuge shows its general southward deepening (Figure 13a). It reaches time depths from 0.29 s TWT at the southern edge of the coal-bearing foreland basin down to 2.86 s TWT south of Cambrai (approximate depth range of 100–6,750 m, based on seismic-well ties). To the north, tight isochrons highlight a steeper dip of the AMBT near the surface, while spread isochrons to the south show a lower dip of the AMBT at depth. A comparison between map traces of the AMBT (black continuous line) and of the basal reflector of the Namurian-Westphalian sequence (dark pink dotted line) points out that the syn-orogenic deposits extend more than 20 km south of the frontal thrust zone below the Ardennes Allochthonous Unit. This configuration basically emphasizes a high degree of localization of displacement on the AMBT.

An important outcome is the lateral evolution of the strike of the AMBT from West (Arras) to East (Maubeuge) (Figure 13a). As mentioned above, the overall orientation of the Northern Variscan Front in northern France-southern Belgium changes laterally from WNW-ESE (N110–120°) in the Boulonnais and Artois regions, to ENE-WSW (N60–70°) in the Avesnois region and the Ardennes Massif. In our study area, these two major trends are visible at depth. South of Valenciennes and Lens, the AMBT trends N70–80° and is orthogonal to the Variscan shortening direction (i.e., SSE–NNW) (Figure 13a). This is consistent with the general strike of the Northern Variscan Front known in this area. Therefore, we consider the direction of Variscan shortening along the AMBT in these regions as frontal. However, south of Douai, the AMBT trends N130° and is almost parallel to the direction of Variscan shortening (Figure 13a). This major change in strike indicates the presence of a lateral thrust ramp relaying the two frontal thrust ramps to the south of Lens and Valenciennes. A second-order lateral ramp, striking N120°, is visible NE of Cambrai. An apparently oblique thrust ramp is also visible further east in the Maubeuge area, where the AMBT trends N110°. Unfortunately, seismic profiles are lacking in the southern part of this area, which would have allowed us to determine the actual trend of the basal thrust.

Another major outcome arising from the 3-D integration of the seismic data is the new map trace of the frontal thrust zone under the Mesozoic-Cenozoic cover between Douai and Valenciennes (Figure 13a). The latter does not represent the original geometry of the frontal thrust zone but its current state. Indeed, the frontal thrust zone continued further north during late Carboniferous times and was eroded afterward. The easily identifiable seismic facies of the AMBT allowed us to accurately interpret its northern extension on the seismic profiles A55, C083, C099, C101, C122, C586, and M146. East of the M146 profile and in the areas with no seismic data, the trace of the AMBT corresponds to the trace of the "Midi Fault" (Figure 1a). Some major changes have been made between Douai and Valenciennes, where seismic data are available. The interpretation of the eastern part of the C586 profile highlighted the presence of two distinct thrusts relaying at the base of the Ardennes Allochthonous Unit. The eastern thrust, trending N70° and characterized by a

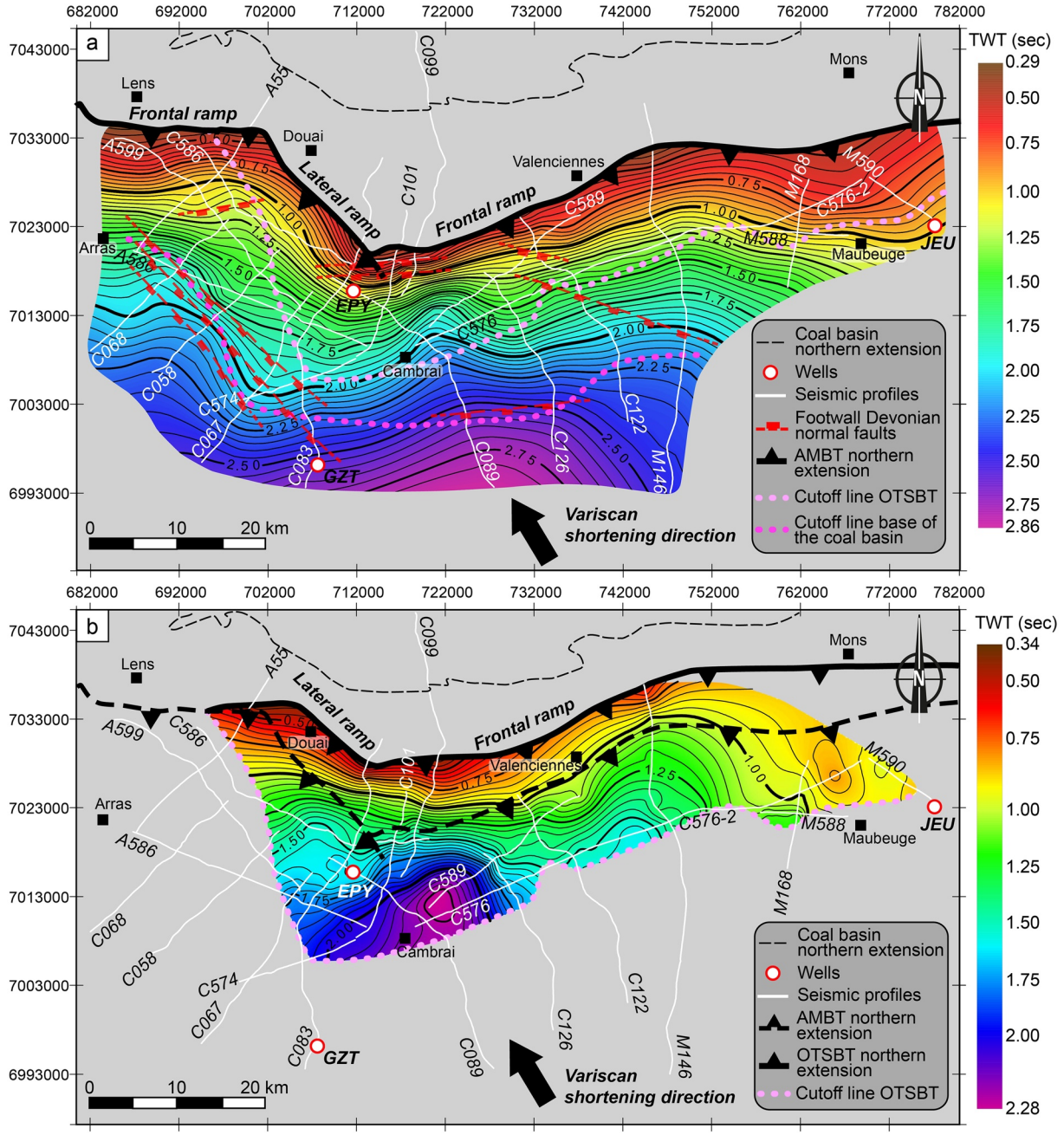

Figure 13. Isochron maps of (a) the Allochthon Main Basal Thrust (AMBT) (grid cell size of 1500 × 1500 meters) and (b) the Overturned Thrust Sheets Basal Thrust (OTSBT) (grid cell size of 500 × 500 meters), computed from seismic interpretation. Contour lines are every 0.05 s. The modeling was carried out using IHS Kingdom Software. Map coordinates are in French Lambert 93. A new outline of the AMBT truncated by the Mesozoic-Cenozoic cover is proposed, based on the results of the seismic interpretation.

frontal ramp geometry south of Valenciennes, is truncated to the west by a second thrust, trending N130° south of Douai (lateral ramp) and N70–80° south of Lens (frontal ramp) (Figure 13a). Therefore, this result indicates that the Northern Variscan Front appears to have a segmented geometry in northern France, rather than a continuous one (Figure 13a). The lateral ramp south of Douai relays two major frontal thrusts of a segmented Northern Variscan Front, trending generally WSW-ENE.

19449194, 2021, 7, Downloaded from https://agupubs.onlinelibrary.wiley.com/doi/10.1029/2020TC006642 by Cochrane France, Wiley Online Library on [13/12/2023]. See the Terms and Conditions (https://onlinelibrary.wiley.com/terms-and-conditions) on Wiley Online Library for rules of use; OA articles are governed by the applicable Creative Commons License

6.2. 3-D Geometry of the OTSBT

The structural map of the OTSBT indicates that this basal thrust deepens southward and reaches depths between 0.34 s TWT in the coal basin and 2.28 s TWT to the south (approximate depth range of 100–5,500 m, based on seismic-well ties), where it intersects the AMBT (Figure 13b). Its cut-off line is represented on the grids of both the AMBT (Figure 13a) and the OTSBT (Figure 13b). A striking feature on this map is the substantial southward extension of the OTS. Indeed, the OTSBT and consequently the OTS extend over 15–25 km between their northern limit in the coal basin and their cut-off line with the AMBT to the south.

Major strike variations are evidenced by the 3-D integration of seismic interpretation between Douai and Maubeuge cities, thus, illustrating the lateral evolution of the OTSBT geometry. To the east (area of Valenciennes), this thrust is orthogonal to the Variscan shortening direction (i.e., SSE–NNW) as it strikes approximatively N70°. It follows therefore the overall structural trend of the Northern Variscan Front in the Avesnois region and the Ardennes Massif (i.e., WSW–ENE). The OTSBT strike changes progressively westward, from WSW–ENE to SE–NW (N110–130°) in the area of Douai. Accordingly, it highlights the transition from a frontal thrust ramp geometry near Valenciennes to an oblique and lateral thrust ramp geometry southeast of Douai. Local changes in strike are visible in a few areas. The transverse structure seems to be transferred east of Cambrai into a rather steep about N160 ramp as observed at the western end of the C576 profile (Figure 11). The related abrupt deepening delimits eastward a zone of maximum depth of the OTSBT, whereas it appears to be bounded by a N070 trending ramp along its northern border (close to the Epinoy borehole). Another lateral thrust ramp can be identified northwest of Maubeuge, where the OTSBT trends about N130°. However, seismic data crossing the thrust front at the eastern end of the study area are lacking and a precise description of the 3–D geometry in this area is not possible.

An interesting correlation appears when comparing the 3-D geometries of both the AMBT and the OTSBT. The lateral or oblique ramps of both thrusts are superimposed, as well as the frontal ramps. For instance, the second-order lateral ramp of the AMBT northeast of Cambrai, is superimposed to the lateral ramp of the OTSBT identified in this area (Figure 11). Likewise, the strike-deviation zone between Douai and Valenciennes coincides geographically with that of the AMBT, presented above (Figure 13a). This finding is important because it shows that both of these out-of-sequence thrusts were deformed along the same two main axes between Lens and the Belgian border. The first axis (N60–70°) is orthogonal to the Variscan shortening direction in the area of Valenciennes, whereas the second one (N110–130°) is parallel or oblique to the Variscan shortening direction in the areas of Douai, Maubeuge and northeast of Cambrai.

6.3. 3-D Geometry of the Southern Laurussian Margin

We computed a structural map of the top-Givetian limestone sequence at the base of the Brabant Para-autochthonous Unit (Figure 14). This map is the first 3-D image showing the structure of the underthrust, slightly deformed southern Laurussian margin in northern France. This map shows that the Givetian carbonates are present at a depth between 0.29 and 3.47 s TWT (approximate depth range of 50–8,500 m, based on seismic-well ties). They generally gently deepen southward in response to the thrust-loading flexural bending of the Brabant Parautochthonous Unit. To the north, in the coal basin area, the Middle Devonian carbonate sequence displays a steeper monoclinal geometry, as shown by the tightened and parallel isochrons. It strikes N120–130° in the area of Douai and N70° north of Valenciennes. South of the coal basin area, the southern Laurussian margin has a more irregular geometry as emphasized by the 3-D geometry of the top Givetian reflector. Between Maubeuge and Cambrai, it slowly deepens towards the south-west and is characterized by an alternation of quite flat levels with steeper-dipping levels, defining a staircase geometry striking around N130°. Between Lens and Cambrai, the southern Laurussian margin has an overall N50° orientation and deepens towards the south-east.

Seismic interpretation has shown that the Brabant Para-autochthonous Unit is deformed by major deep structures (both compressional and extensional) south of the coal basin area. Some of them have been correlated from line to line and are illustrated on the structural map of the Givetian top (Figure 14). Between Arras and Cambrai, the top-Givetian reflector is affected by a pair of anticline and syncline (orange folds axes) striking N120–130°. Those folds correspond to the deep anticline and associated syncline interpreted on the C083 seismic profile (Figure 10).

19449194, 2021, 7, Downloaded from https://agupubs.onlinelibrary.wiley.com/doi/10.1029/2020TC006642 by Cochrane France, Wiley Online Library on [13/12/2023]. See the Terms and Conditions (https://onlinelibrary.wiley.com/terms-and-conditions) on Wiley Online Library for rules of use; OA articles are governed by the applicable Creative Commons License

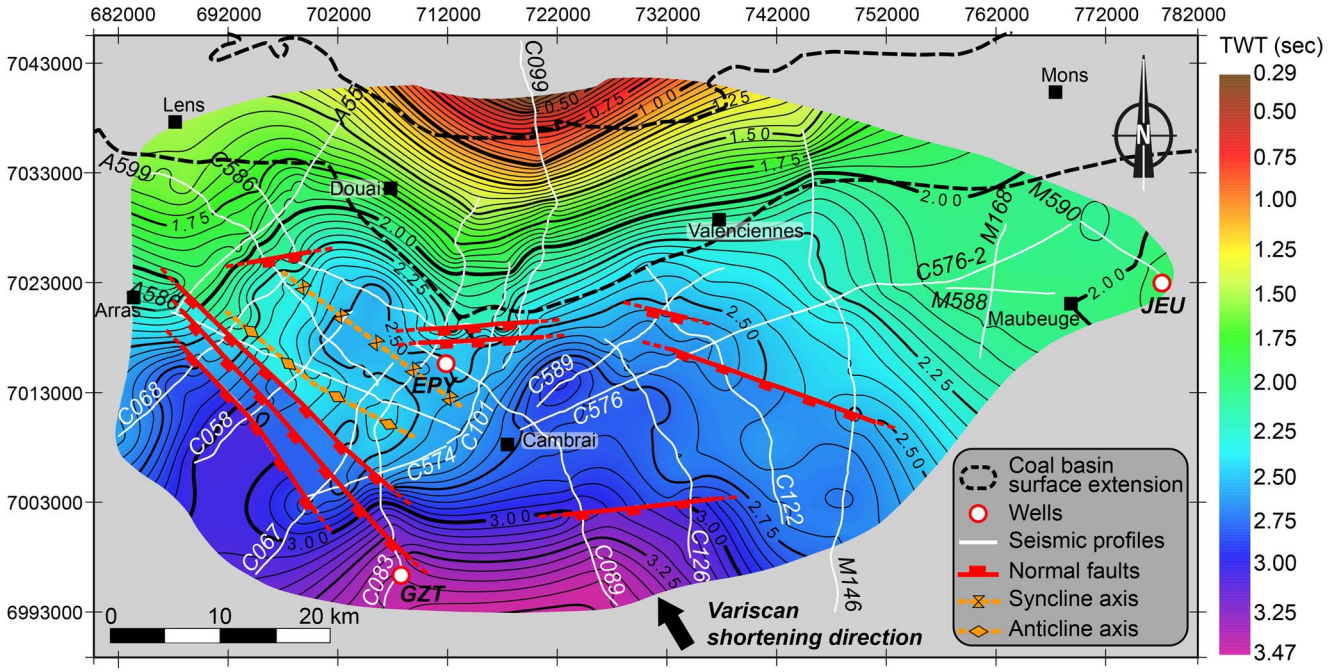

Figure 14. Isochron map of the top of the Givetian (grid cell size of 100 × 100 meters). This structural grid was modeled based on the seismic interpretation of the Givetian top. The modeling was carried out using IHS Kingdom Software. Equidistance is 0.05 s. Map coordinates are in French Lambert 93.

The syn-sedimentary normal faults inherited from the pre-orogenic Laurussian margin deformation have also been laterally correlated and illustrated on the structural map (Figure 14). In detail, three different sets of faults strikes can be distinguished from the east to west: a) N120° south of Valenciennes, b) N130° south of Douai-Lens and c) about N70–80° in the central region. Considering that the N120° and N130° striking sets cannot be regarded as significantly different fault systems, it can be inferred that the southern Laurussian margin was basically segmented by a system of normal faults striking N70–80° and N120–130°. This finding is consistent with previous studies that suggest that the Laurussian margin in northern France-southern Belgium was segmented by a set of N50–70° and N110–130° trending normal faults during the syn-rift Devonian stage (e.g., Meilliez et al., 1991; Lacquement, 2001). These syn-sedimentary normal faults have significantly contributed to the southward deepening of the southern Laurussian margin and the associated thickening of the Devonian series. It is particularly visible southeast of Arras, where the N130-trending normal faults are characterized by an important down-dip throw responsible for the substantial deepening of the Devonian layers towards the south-west and the associated thickening of the Upper Devonian sequence (Figure 9).

The superposition of Variscan structures and pre-existing Devonian normal faults is well illustrated in 3-D on the structural map of the AMBT (Figure 13a). Except for the region located south of Valenciennes, the geometry of the AMBT follows the strike of the Devonian normal faults in its footwall. Furthermore, comparison of the structural maps of the AMBT (Figure 13a) and OTSBT (Figure 13b) to the structural map of the Givetian top (Figure 14) reveals a spatial correlation between the geometry of the Variscan thrusts and the topography of the Devonian substratum in the footwall of these faults. Indeed, frontal thrust ramps of the AMBT (Figure 13a) and OTSBT (Figure 13b) developed where the rifted Laurussian margin was trending N60–80° and deepened southeastward, while the lateral and oblique thrust ramps developed, trending N110–130° and deepening southwestward. For instance, the N130° trend of the lateral ramp of the AMBT south of Douai matches the trend of the underlying Laurussian rifted margin. The strike-deviation zone between Douai and Valenciennes coincides with a major change in orientation of the underlying substratum. Northeast of Cambrai, the superimposed lateral ramps of the AMBT and OTSBT, both visible on the seismic data (Figure 11) and structural maps, developed above the edge of a topographic trough, trending SE-NW. Overall, the main Variscan thrusts seem to be molded on the topography of the Laurussian margin inherited from the Devonian Rheno-Hercynian extensional event.

19449194, 2021, 7, Downloaded from https://agupubs.onlinelibrary.wiley.com/doi/10.1029/2020TC006642 by Cochrane France, Wiley Online Library on [13/12/2023]. See the Terms and Conditions (https://onlinelibrary.wiley.com/terms-and-conditions) on Wiley Online Library for rules of use; OA articles are governed by the applicable Creative Commons License

19449194, 2021, 7, Downloaded from https://agupubs.onlinelibrary.wiley.com/doi/10.1029/2020TC006642 by Cochrane France, Wiley Online Library on [13/12/2023]. See the Terms and Conditions (https://onlinelibrary.wiley.com/terms-and-conditions) on Wiley Online Library for rules of use; OA articles are governed by the applicable Creative Commons License

7. Discussion

7.1. New Insights on the Geometry of the Northern Variscan Front in Northern France

Our seismic interpretation provides a new understanding of the 3-D geometry of the North Variscan Front in northern France, so far locally described from 2-D geological cross-sections. The along-strike lateral changes in the geometry of the thrust front and its controlling factors are discussed below.

7.1.1. Segmentation of the Thrust Front

Study of the 3-D geometry of the two main thrusts of the Northern Variscan Front (AMBT and OTSBT) demonstrates the existence of major lateral ramps south of Douai, relaying two frontal thrust segments: the first one located south of Valenciennes, and the second one south of Lens (Figure 13). This new finding corroborates several studies (Averbuch et al., 2002; Lacquement, 2001; Lacquement et al., 2005; Mansy & Meilliez, 1993; Meilliez, 1989; Raoult, 1986) that suggest that the zones of major change in strike observed along the Northern Variscan Front of NW Europe correspond to lateral or oblique thrust ramps relaying several major thrusts of a segmented front.

At a smaller scale, some previous studies focusing on a similar change in strike in the Meuse valley-Dinant recess (Ardennes Massif) (Lacquement et al., 2005; Szaniawski et al., 2003) have suggested that these lateral and oblique ramps, including the one located south of Douai, may have acted as transfer zones during the propagation of the thrust front in late Carboniferous times. They would have localized transpressional corridors that accommodated components of both right-lateral strike-slip deformation and oblique shortening. Such a process was evidenced by analog modeling experiments (e.g., Martinez et al., 2002; McClay et al., 2004) showing that convergence oblique with respect to the margin can lead to strain partitioning between margin-normal contraction and margin parallel strike-slip faulting. This could apply south of Douai where the Laurussian margin is parallel-to-oblique with respect to the direction of the Variscan shortening (Figure 14). The transverse shortening localized along the lateral ramps evidenced on the C576 seismic profile (Figure 11) is likely to reflect such transpressional deformation partitioned between different faults.

7.1.2. Structural Inheritance

Results of the seismic interpretation showed that Variscan thrust ramps localized above Devonian normal faults, therefore suggesting that these pre-existing extensional structures acted as areas of preferential nucleation of the subsequent contractional thrust ramps. We argue that such basement discontinuities focused contractional stress during the northward propagation of the thrust front in Late Mississippian-Middle Pennsylvanian and consequently had a buttressing effects that controlled the nucleation of subsequent thrust ramps. This phenomenon has been observed and described already in the 1980s (Butler, 1989; Gillcrist et al., 1987; Schedl & Wiltschko, 1987; Wiltschko & Eastman, 1983) in various fold-and-thrust belts, especially in the Appalachians (Konstantinovskaya et al., 2014; Thomas, 2001, 2007), in the Apennines (Butler et al., 2006; Scisciani, 2009; Tavarnelli, 1996, 1999), in the Jura Mountains (Malz et al., 2020; Ustaszewski & Schmid, 2006), in the Alps (Butler et al., 2006), in the Himalayas (Butler, 2020), and at the eastern end of the Variscan deformation front in Poland (Krzywiec et al., 2017; Kufrasa et al., 2020), among others. The structure of the Northern Variscan Front in northern France provides a new example of the control exerted by inherited extensional basement structures on the deformation of a propagating thrust front.

At a regional scale, structural maps reveal that the 3-D geometry of the main Variscan thrusts (AMBT and OTSBT) (Figure 13) can be correlated to the topography of the underlying rifted structures of the Laurussian margin (Figure 14). Results show that the major lateral ramps of the AMBT and OTSBT south of Douai formed above the SW-deepening Laurussian margin segmented by N130° striking Devonian normal faults, parallel to the shortening direction. Various natural case studies (Amadori et al., 2019; Lacombe et al., 2003; Lacquement et al., 2005; Paulsen & Marshak, 1999; Ustaszewski & Schmid, 2006), and analog modeling experiments (e.g., Calassou et al., 1993) have emphasized the significant control exerted by inherited basement topography on the geometry and segmentation of thrust fronts along-strike, especially by localizing lateral or oblique ramps, salients and reentrants. Examples in the Jura Mountains (France) (Ustaszewski & Schmid, 2006), in the Sevier fold-thrust belt (Utah, USA) (Paulsen & Marshak, 1999) or in Taiwan (Lacombe et al., 2003) have shown that lateral or oblique thrust ramps of a propagating thrust front are likely to form above basement offsets (often fault-related) trending parallel or oblique with respect to the shortening

direction. By localizing both Variscan frontal and lateral ramps, the inherited structure of the southern Laurussian margin had a major impact on the 3-D geometry and along-strike segmentation of the Northern Variscan Front.

7.2. Synthesis of the Kinematic Evolution of the Northern Variscan Front in Northern France

Results of our seismic interpretation emphasize the main tectonic features of the Northern Variscan Front in northern France. We aim now at providing a regional scope to the structural and kinematic model of the thrust front previously described on the basis of local studies in the Valenciennes (M146 seismic profile, Figure 3) (Averbuch et al., 2018; Lacquement, 2001; Lacquement et al., 1999; Mansy et al., 1997) and Artois regions (Minguely et al., 2008) and attempt an unprecedented regional synthesis of the kinematic evolution of the Northern Variscan Front in northern France. It takes into account known elements from previous studies on the thrust front, as well as additional contributions from our study, in particular (a) the quantification of the regional underthrusting of the foreland basin, (b) the deep folding and thrusting of the Brabant Para-autochthonous Unit, and (c) the nucleation of thrusts ramps above pre-existing basement faults. We present and detail a new conceptual tectonic model for the kinematic evolution of the thrust front showing the successive stages of deformation during the Late Mississippian-Middle Pennsylvanian (Figure 15). The evolution is divided into seven stages (from A to G), with A representing the early compressional stage of the Variscan foreland (Late Mississippian), and F the last compressional stage (Middle Pennsylvanian); stage G depicts the present-day situation. The specific tectonic features of the thrust front visible on this model are discussed below.

7.2.1. Localized Displacement of the Ardennes Allochthonous Unit Onto the AMBT

Our seismic interpretation has emphasized the high degree of localization of displacement onto the AMBT during the Variscan shortening stage. First-time regional quantification of the relative underthrusting of the foreland basin revealed the latter extends on average 20–25 km southward below the Ardennes Allochthonous Unit (Figure 13a). Based on the restoration of the M146 seismic section (Figure 3), and corroborated by the seismic profiles trending almost parallel the average transport direction presented above (Figures 7 and 8), a total displacement of at least 50 km can be estimated along the AMBT (stage F, Figure 15). However, these values are likely to be underestimated, considering that the thrust front extended further north in late Carboniferous times and was later eroded (stage G, Figure 15).

Similar examples of thrusts localizing important displacement exist in various fold-and-thrust belts. In the Southern Apennines (Italy), the Lagronegro allochthon accommodated more than 65 km of displacement (Butler, 2020; Butler et al., 2004), resulting in the large underthrusting of the Apulian foreland. In the Central Salt Range (Pakistan), the Salt Range Thrust localized about 25 km of displacement (Butler, 2020; Qayyum et al., 2015). Numerous studies based on analog modeling and studies of natural cases, argue that syn-kinematic sedimentation exerts a strong influence on the structural evolution of a thrust wedge (e.g., Storti & McClay., 1995; Barrier et al., 2002; Bonnet et al., 2008; Wu & McClay, 2011; Graveleau et al., 2012). Butler (2020) showed that if there is little or no sedimentation at the toe of an emergent thrust front, an individual emergent thrust having a low-angle dip can localize a large amount of slip and carry thrust allochthons, therefore creating a significant sub-thrust or underthrust foreland. If the sedimentation rate increases at the thrust front, the emergent thrust may steepen significantly therefore reducing its tendency to slip. Consequently, deformation may be transferred onto new additional structures in the thrusts hangingwall and footwall.

We, therefore hypothesize that surface processes may have had a significant influence on the geometry of the Northern Variscan Front in northern France. A low sedimentation rate at the toe of the propagating AMBT would provide a viable explanation for the high degree of localization of displacement on the AMBT (stages B and C, Figure 15). This would be consistent with the low-angle dip of the AMBT visible south of the frontal thrust zone (Figure 13a) and at the southern end of the seismic profiles. A later increase in sedimentation rate in the foreland basin may have had a significant influence on the steepening of the AMBT in the frontal thrust zone (Figure 13a), evolving from a footwall flat geometry with large displacement into a footwall ramp geometry with lower displacement (stages D, E, F, Figure 15).

19449194, 2021, 7, Downloaded from https://agupubs.onlinelibrary.wiley.com/doi/10.1029/2020TC006642 by Cochrane France, Wiley Online Library on [13/12/2023]. See the Terms and Conditions (https://onlinelibrary.wiley.com/terms-and-conditions) on Wiley Online Library for rules of use; OA articles are governed by the applicable Creative Commons License

10.1029/2020TC006642

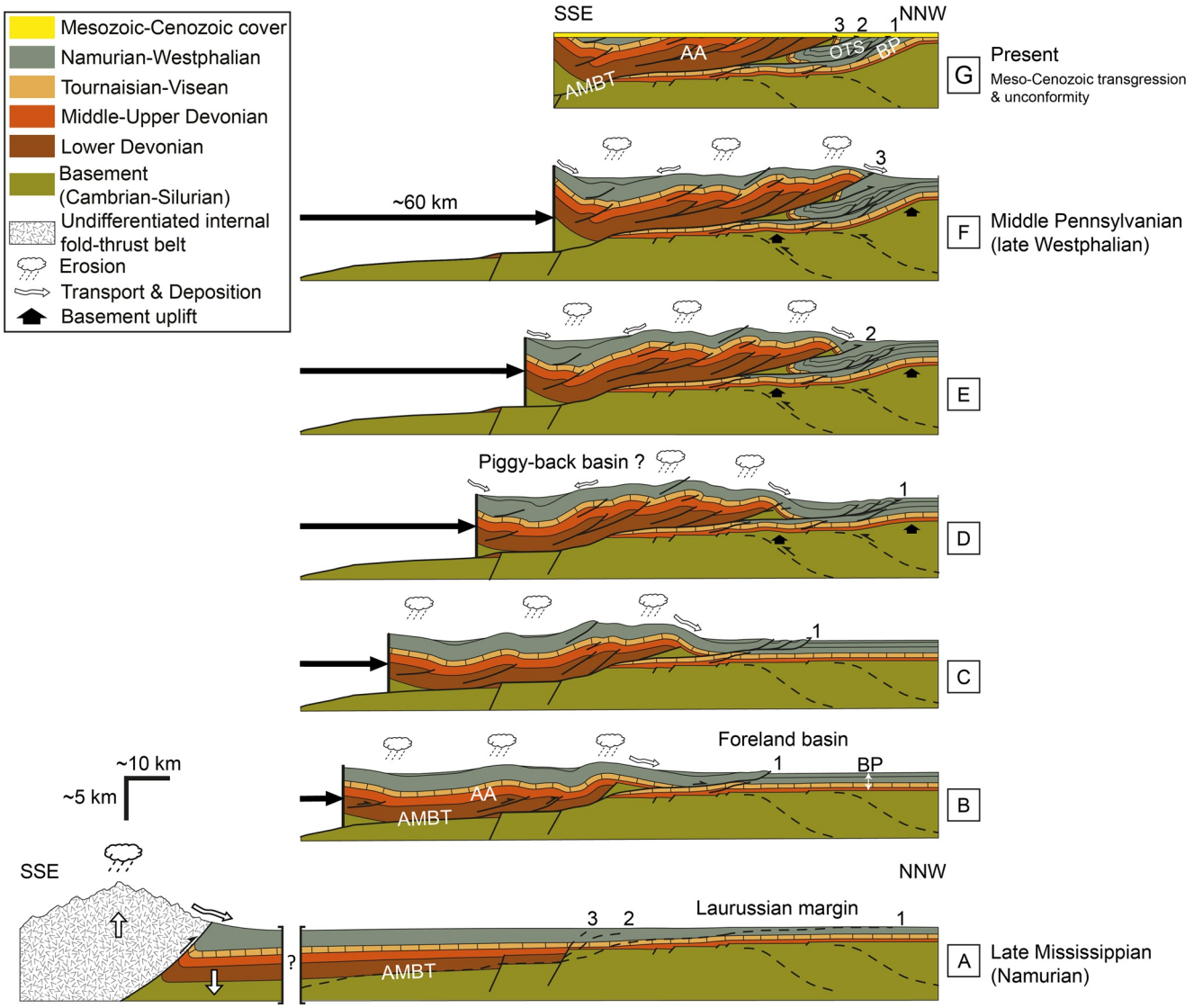

Figure 15. Conceptual kinematic model of the Northern Variscan Thrust Front in northern France (segment to the east of the Douai lateral ramp), integrating previous work (see Figure 3) and new insights from the present study. AA: Ardennes Allochthonous Unit, AMBT: Allochthon Main Basal Thrust, BP: Brabant Para-autochthonous Unit, OTS: Overturned Thrust Sheets. Numbers 1, 2 and 3 correspond to the order of activation of the different thrust faults, the OTSBT, the "Cran de Retour" thrust and the "Midi Fault," illustrating the out-of-sequence deformation sequence of the Northern Variscan Front during late Westphalian times.

7.2.2. Out-Of-Sequence Dislocation of the Thrust Front

The detailed interpretation of the C083 profile (Figure 10 & 12) and the analysis of the structural map of the OTSBT (Figure 13b) demonstrated that the OTS have the overall geometry of a recumbent syncline north of Cambrai and are truncated by the AMBT at least 15 km south of the frontal thrust zone. The overturned limb of this recumbent syncline is likely to correspond to that of a major thrust-related anticline, whose progressive rotation and overturn was induced by the basal shear associated to the large displacement of the Allochthonous Unit on the AMBT (stages C, D, E, F, Figure 15). The existence of such an antiform was established in the "Condroz inlier" of the Belgian Ardennes, along the Meuse River Cross-section (Adams & Vandenberghe, 1999; Khatir et al., 1992; Le Gall, 1992; Raoult & Meilliez, 1987), where lower Paleozoic rocks are exposed. Within the OTS complex, internal strain is likely to have been accommodated by the formation of Riedel-type low-angle normal shear planes of minor scale, as observed in Figure 12 and in the coal-bearing molasse from the NPC basin (e.g., Bouroz, 1950; Le Gall, 1994; Meilliez, 2019). This kind of

19449194, 2021, 7, Downloaded from https://agupubs.onlinelibrary.wiley.com/doi/10.1029/2020TC006642 by Cochrane France, Wiley Online Library on [13/12/2023]. See the Terms and Conditions (https://onlinelibrary.wiley.com/terms-and-conditions) on Wiley Online Library for rules of use; OA articles are governed by the applicable Creative Commons License

19449194, 2021, 7, Downloaded from https://agupubs.onlinelibrary.wiley.com/doi/10.1029/2020TC006642 by Cochrane France, Wiley Online Library on [13/12/2023]. See the Terms and Conditions (https://onlinelibrary.wiley.com/terms-and-conditions) on Wiley Online Library for rules of use; OA articles are governed by the applicable Creative Commons License

structures represent relatively uncommon objects in mountain fronts and foreland basins but they were described in highly strained zones below forelimb thrusts in different foreland fold-thrust structures (i.e., the Jura, NE Pyrenees, Central Apennines) (Averbuch et al., 1992, 1995; Smeraglia et al., 2020). The particularly large horizontal simple-shear strain associated with the forward rotation of the forelimb of the thrust-related anticline developed above the frontal ramp of the AMBT is likely to account for the unusual mechanical conditions controlling the generation of such a low-angle normal fault (Frizon de Lamotte et al., 1995).

The anticline was sequentially cross-cut by out-of-sequence forelimb thrusts, identified in the region as the "Cran de Retour" thrust (2 in Figure 15) and the "Midi Fault" (3 in Figure 15), the latter being the last out-of-sequence thrust (stages D, E, F, Figure 15). Such an out-of-sequence dislocation of the frontal thrust zone can be explained in different ways. It may evidence an impossibility of the thrust front to propagate further north due to, for instance, an uplift of the Brabant Massif that acted as a buttress located in front of the propagating Variscan thrust wedge (Averbuch et al., 2004; Mansy et al., 1999). This mechanism is a feature predicted by analog modeling of basement asperity subduction (Dominguez et al., 2000; Lallemand et al., 1992). This could partly explain the observed re-entrant of the thrust front rearward of the deep Orchies anticline (Marshak, 2004). Such a mechanical locking is known in other natural cases as in the Central Sivas Basin (Turkey) where a topographic high, the crustal Kirshehir block, limited the propagation of the deformation front, resulting in a structural uplift of the fold-thrust belt through an antiformal stack (Legeay et al., 2020). Alternatively, the influence of large volume of syntectonic sedimentation in front of the active thrust front may have led to a backward sequence of thrusting and steepening of the thrust sheet (Barrier et al., 2002; Butler, 2020).

7.2.3. Variscan Reactivation of the Front of the Anglo-Brabant Deformation Belt

Seismic interpretations (C083 profile, Figure 10) and analysis of the structural map of the top-Givetian horizon (Figure 14) revealed the existence of a N120–130 trending deep anticline-syncline pair of folds within the Brabant Para-autochthonous Unit, west of Cambrai. Accounting for the close proximity of the Northern Variscan Front and the late Caledonian Anglo-Brabant deformation belt in the study area (Mansy et al., 1999; Pharaoh, 2018; Pharaoh et al., 1993; Van Grootel et al., 1997), we suggest that this deep anticline may have accommodated shortening associated with the Variscan reactivation of south-vergent thrusts of the Anglo-Brabant deformation front buried within the basement (stages D to F, Figure 15). This hypothesis is supported by the orientation of the WNW-ESE main structural trend of the Anglo-Brabant deformation belt (Mansy et al., 1999; Pharaoh, 2018; Pharaoh et al., 1993; Van Grootel et al., 1997). The pronounced flexure and monoclinal geometry of the Brabant Para-autochthonous Unit delimiting to the north the foreland basin (Figure 14), could possibly have the same origin (Figure 15).

The poor quality of the seismic data in the basement does not allow imaging the deep late Caledonian thrusts. Such structures have, however, been observed on seismic data further west in the Artois region (Minguely et al., 2008) (location in Figure 1a). In this area, north-verging Variscan thrusts and south-verging basement thrusts, interpreted as possible frontal thrusts of the Anglo-Brabant fold belt, form a peculiar frontal triangle zone that uplifted the foreland. Analog modeling experiments conducted for the Artois region (Minguely et al., 2008) and the northern Apennines (Toscani et al., 2014) investigated the mechanism of deformation of two interfering thrust fronts having opposite vergence. Results showed that the pre-existing thrusts (i.e., the late Caledonian thrusts) seems to be reactivated once the northern tip of the younger propagating thrust wedge (i.e., the Variscan thrust wedge) reached the pre-existing thrust front (i.e., the Anglo-Brabant thrust front). Analog modeling experiments (Minguely et al., 2008) argue that the reactivation of such deep inherited thrusts, forming part of a deep frontal triangle zone and resulting in the relative uplift of the Brabant foreland, would have exerted a major buttressing effect in front of the northward propagating Variscan thrust front. Such a process is likely to have enhanced both the localization of displacement on the single AMBT and the out-of-sequence dislocation of the hangingwall anticline developed previously at the tip of the propagating thrust front (stages D to F, Figure 15). Similar cases have been observed in emergent fold-and-thrust belts in the Alps (Ortner et al., 2015) or the Andes (Calderon et al., 2017). For example in the Alps (western Austria, southern Germany), the formation of a frontal triangle zone stopped the foreland propagation of the Alpine thrust front and initiated a break-back sequence of thrusting into the hinterland (Ortner et al., 2015).

8. Conclusions

Seismic profiles presented in this article show the 3-D structure and kinematics of the Northern Variscan Thrust Front in northern France. The frontal thrust zone (AMBT) is shown to localize the displacement of the Ardennes Allochthonous Unit over more than 50 km above the Laurussian margin referred here as the Brabant Para-autochthonous Unit. This large displacement induced underthrusting of the molassic foreland basin and its truncation by a major out-of-sequence thrust (the shallow part of the AMBT, frequently referred to as the Midi fault). An extensive complex of dominantly overturned thrust sheets (the OTS complex) at the sole of this thrust, is interpreted as the result of dissection of a previous major hangingwall anticline at the tip of the AMBT, its forelimb being successively cross-cut and overturned by basal shear along the footwall of the propagating out-of-sequence major thrust.

A major outcome of our 3-D approach is the characterization of a major NW-SE-trending lateral ramp, approximatively along a line Douai-Cambrai and that affects both the main frontal thrust (AMBT) and the OTSBT. This deep-seated ramp marks the western extent of the OTS complex. This is a major relay zone along the thrust front in between the eastern segment (trending ENE-WSW between Valenciennes and Douai), where the molassic foreland basin is largely underthrust (more than 20 km) below the Allochthonous Unit, and the western segment (trending WNW-ESE in the Boulonnais and Artois regions) where no underthrusting occurred. The way this transfer zone is accommodated in the foreland basin is poorly known and thus remains a major objective for future research.

Another key result is the 3-D characterization of the Brabant Para-autochthonous Unit. Along with the overlying Namurian-Westphalian synorogenic layers trapped in the Northern Variscan foredeep, these are deformed by a series of second-order north-verging thrust faults often associated with ramp-related folds developed at their hangingwall. The transition zones between (a) the Famennian shales and the underlying Frasnian limestones, and (b) the Namurian shales and the Dinantian carbonates form the main décollements within this unit.

We showed that at the base of the Brabant Para-autochthonous Unit, the Middle-Upper Devonian sequence has been deformed by syn-sedimentary normal faults. Those faults are responsible for the general thickening of the Devonian sequence towards the south or southwest. Their N060–080° and N110–130° trend corresponds precisely to the strike of the frontal and lateral ramps of the Variscan thrust wedge. Our seismic interpretations also confirm that numerous Variscan thrusts formed right above the Devonian syn-sedimentary normal faults. This observation is valid for both the frontal and lateral ramps and points out the impact of mechanical heterogeneities on the localization of later thrust ramps. Indeed, rift-related deformation in the southern Laurussian margin has exerted a major control on the dynamics of the thrust front by controlling the spacing between individual thrusts, the frictional conditions at the base of the thrust wedge and its along-strike segmentation.

Seismic interpretations revealed the presence of deep folds within the underthrust foreland affecting both the Para-autochthonous Unit and its lower Paleozoic substratum. We propose that their origin is associated with the activation of a deep-seated early Paleozoic backthrust in the basement. The pronounced flexure delimiting to the north the coal-bearing foreland basin and exhuming the lower Paleozoic basement could possibly have the same origin. Such deep foreland back-thrusts are likely to have exerted a major buttressing effect in front of the northward propagating Variscan thrust front, thereby possibly enhancing its out-of-sequence dislocation and the localization of slips along one single major thrust (i.e., the AMBT).

Finally, we propose a conceptual tectonic scenario that fits the main geometric and kinematic characteristics of the Variscan frontal thrust zone in northern France. Hopefully this scenario should benefit from further input of new field and subsurface data, and thus remains to be explored to better constrain the kinematic evolution of this ancient mountain front.

Data Availability Statement

According to French laws, the field seismic data are publically available at http://www.minergies.fr/fr. The reprocessed seismic data (SEG-Y) used in this paper belong to the BRGM, so they can be released only with a formal agreement with the BRGM.

19449194, 2021, 7, Downloaded from https://agupubs.onlinelibrary.wiley.com/doi/10.1029/2020TC006642 by Cochrane France, Wiley Online Library on [13/12/2023]. See the Terms and Conditions (https://onlinelibrary.wiley.com/terms-and-conditions) on Wiley Online Library for rules of use; OA articles are governed by the applicable Creative Commons License

Acknowledgments
This work is part of the Ph.D. thesis of Aurore Laurent, granted by the BRGM (French Geological Survey) and the Hauts-de-France region. It is based on the interpretation of 21 seismic lines reprocessed by the BRGM. The reprocessing of the seismic data was supported by the RGF program of the BRGM. Eight lines are presented in the paper, the others are not, but all of them have been used to produce the interpretations and maps presented here.
This work benefitted also from a financial support from the TelluS Program of the CNRS/INSU. IHS Markit is greatly acknowledged for the permission to use the Kingdom Suite software through an academic grant to the University of Lille. We also thank QGIS development team for providing the QGIS open-source software used during this study. The authors gratefully acknowledge the Editor L. Jolivet, the Associate Editor O. Lacombe and the reviewers P. Krzywiec, S. Mazur and an anonymous reviewer for their constructive comments that significantly improved the manuscript. We particularly thank B. Vendeville for his careful reading of this article and help in the improvement of the English style.

References

Adams, R., & Vandenberghe, N. (1999). The Meuse section across the Condroz–Ardennes (Belgium) based on a predeformational sediment wedge. *Tectonophysics*, *309*(1–4), 179–195. https://doi.org/10.1016/S0040-1951(99)00138-9

Allen, P. A., Homewood, P., & Williams, G. D. (1986). Foreland Basins: An Introduction. In P. A. Allen, & P. Homewood (Eds.), Foreland basins. Special Publication of the International association of Sedimentologists (Vol. 8, pp. 3–12). Blackwell Scientific Publications.

Amadori, C., Toscani, G., Di Giulio, A., Maesano, F. E., D'Ambrogi, C., Ghielmi, M., & Fantoni, R. (2019). From cylindrical to non-cylindrical foreland basin: Pliocene–Pleistocene evolution of the Po Plain–Northern Adriatic basin (Italy). *Basin Research*, *31*(5), 991–1015. https://doi.org/10.1111/bre.12369

Averbuch, O., Frizon de Lamotte, D., & Kissel, C. (1992). Magnetic fabric as a structural indicator of the deformation path within a fold-thrust structure: A test case from the Corbières (NE Pyrenees, France). *Journal of Structural Geology*, *14*(4), 461–474. https://doi.org/10.1016/0191-8141(92)90106-7

Averbuch, O., Frizon de Lamotte, D., & Kissel, C. (1993). Strain distribution above a lateral culmination: An analysis using microfaults and magnetic fabric measurements in the Corbières thrust belt (NE Pyrenees, France). *Annales Tectonicae*, *7*(1), 3–21.

Averbuch, O., Lacquement, F., Meilliez, F., Graveleau, F., Beccaletto, L., & Vendeville, B. (2018). *La chaîne varisque vue depuis son front nord: Dynamique du front de chaîne, sous-charriage crustal de la marge avalonienne et délamination associée de la lithosphère supra-subduction*. 26th Réunion des Sciences de la Terre, October 22, 2018.

Averbuch, O., Lacquement, F., Szaniawski, R., Mansy, J. L., & Lewandowski, M. (2002). Segmentation of the Variscan thrust front (N France, S Belgium): Insights into the geometry of the Devonian Rheno-Hercynian Basin. *Aardkundige Mededelingen*, *12*, 89–92.

Averbuch, O., Mansy, J.-L., Lamarche, J., Lacquement, F., & Hanot, F. (2004). Geometry and kinematics of the Boulonnais fold-and-thrust belt (N France): Implications for the dynamics of the Northern Variscan thrust front. *Geodinamica Acta*, *17*(2), 163–178. https://doi.org/10.3166/ga.17.163-178

Averbuch, O., Mattei, M., Kissel, C., Frizon de Lamotte, D., & Speranza, F. (1995). Cinématique des déformations au sein d'un système chevauchant aveugle; l'exemple de la Montagna dei Fiori (front des Apennins centraux, Italie). *Bulletin de la Societe Geologique de France*, *166*(5), 451–461. https://doi.org/10.2113/gssgfbull.166.5.451

Averbuch, O., & Piromallo, C. (2012). Is there a remnant Variscan subducted slab in the mantle beneath the Paris basin? Implications for the late Variscan lithospheric delamination process and the Paris basin formation. *Tectonophysics*, *558–559*, 70–83. https://doi.org/10.1016/j.tecto.2012.06.032

Ballèvre, M., Bosse, V., Ducassou, C., & Pitra, P. (2009). Palaeozoic history of the Armorican Massif: Models for the tectonic evolution of the suture zones. *Comptes Rendus Geoscience*, *341*(2–3), 174–201. https://doi.org/10.1016/j.crte.2008.11.009

Bally, A. W., Gordy, P. L., & Stewart, G. A. (1966). Structure, Seismic Data, and Orogenic Evolution of Southern Canadian Rocky Mountains. *Bulletin of Canadian Petroleum Geology*, *14*(3), 337–381. https://doi.org/10.35767/gscpgbull.14.3.337

Banks, C. J., & Warburton, J. (1986). 'Passive-roof' duplex geometry in the frontal structures of the Kirthar and Sulaiman mountain belts, Pakistan. *Journal of Structural Geology*, *8*(3–4), 229–237. https://doi.org/10.1016/0191-8141(86)90045-3

Barrier, L., Nalpas, T., Gapais, D., Proust, J. N., Casas, A., & Bourquin, S. (2002). Influence of syntectonic sedimentation on thrust geometry. Field examples from the Iberian Chain (Spain) and analogue modeling. *Sedimentary Geology*, *146*(1–2), 91–104. https://doi.org/10.1016/S0037-0738(01)00168-3

Becq-Giraudon, J.-F. (1983). *Synthèse structurale et paléogéographique du bassin houiller du Nord et du Pas-de-Calais. Mémoire BRGM* (No. 123). Editions du BRGM.

Belanger, I., Delaby, S., Delcambre, B., Ghysel, P., Hennebert, M., Laloux, M., et al. (2012). Redéfinition des unités structurales du front varisque utilisées dans le cadre de la nouvelle Carte géologique de Wallonie (Belgique). *Geologica Belgica*, *15*(3), 169–175.

Bonnet, C., Malavieille, J., & Mosar, J. (2008). Surface processes versus kinematics of thrust belts: Impact on rates of erosion, sedimentation, and exhumation – Insights from analogue models. *Bulletin de la Societe Geologique de France*, *179*(3), 297–314. https://doi.org/10.2113/gssgfbull.179.3.297

Bouroz, A. (1950). Sur quelques aspects du mécanisme de la déformation tectonique dans le bassin houiller du Nord de la France. *Annales de la Societe Geologique du Nord*, *70*, 2–55.

Bouroz, A. (1969). Le Carbonifère du Nord de la France. *Annales de la Societe Geologique du Nord*, *89*(1), 47–65.

Bouroz, A., Chalard, J., Dalinval, A., & Stiévenard, M. (1961). La structure du bassin houiller du Nord de la région de Douai à la frontière Belge. *Annales de la Societe Geologique du Nord*, *81*, 173–218.

Bouroz, A., Stièvenard, M., Buisine, M., Chalard, J., Dalinval, A., Dollé, P., et al. (1963). *Houillères du Bassin du Nord et du Pas-de-Calais: Carte des zones stratigraphiques à la cote -300*. Institut Géographique National.

Boyer, S. E., & Elliott, D. (1982). Thrust Systems. *AAPG Bulletin*, *66*(9), 1196–1230. https://doi.org/10.1306/03B5A77D-16D1-11D7-8645000102C1865D

Bultynck, P., Coen-Aubert, M., Dejonghe, L., Godefroid, J., Hance, L., Lacroix, D., et al. (1991). Les formations du Dévonien moyen de la Belgique. *Mémoires pour servir à l'Explication des Cartes Géologiques et Minières de la Belgique*, *30*, 1–106.

Burgess, P. M., & Gayer, R. A. (2000). Late Carboniferous tectonic subsidence in South Wales: Implications for Variscan basin evolution and tectonic history in SW Britain. *Journal of the Geological Society*, *157*(1), 93–104. https://doi.org/10.1144/jgs.157.1.93

Butler, R. W. H. (1982). The terminology of structures in thrust belts. *Journal of Structural Geology*, *4*(3), 239–245. https://doi.org/10.1016/0191-8141(82)90011-6

Butler, R. W. H. (1987). Thrust sequences. *Journal of the Geological Society*, *144*(4), 619–634. https://doi.org/10.1144/gsjgs.144.4.0619

Butler, R. W. H. (1989). The influence of pre-existing basin structure on thrust system evolution in the Western Alps. *Geological Society, London, Special Publications*, *44*(1), 105–122. https://doi.org/10.1144/GSL.SP.1989.044.01.07

Butler, R. W. H. (2020). Syn-kinematic strata influence the structural evolution of emergent fold–thrust belts. *Geological Society, London, Special Publications*, *490*(1), 57–78. https://doi.org/10.1144/SP490-2019-14

Butler, R. W. H., Bond, C. E., Cooper, M. A., & Watkins, H. (2018). Interpreting structural geometry in fold-thrust belts: Why style matters. *Journal of Structural Geology*, *114*, 251–273. https://doi.org/10.1016/j.jsg.2018.06.019

Butler, R. W. H., Mazzoli, S., Corrado, S., Donatis, M. D., Bucci, D. D., Gambini, R., et al. (2004). Applying Thick-skinned Tectonic Models to the Apennine Thrust Belt of Italy–Limitations and Implications. In K. R. McClay (Ed.), Thrust tectonics and hydrocarbon systems (Vol. 82, pp. 647–667). AAPG Memoir. https://doi.org/10.1306/m82813c34

Butler, R. W. H., Tavarnelli, E., & Grasso, M. (2006). Structural inheritance in mountain belts: An Alpine–Apennine perspective. *Journal of Structural Geology*, *28*(11), 1893–1908. https://doi.org/10.1016/j.jsg.2006.09.006

19449194, 2021, 7, Downloaded from https://agupubs.onlinelibrary.wiley.com/doi/10.1029/2020TC006642 by Cochrane France, Wiley Online Library on [13/12/2023]. See the Terms and Conditions (https://onlinelibrary.wiley.com/terms-and-conditions) on Wiley Online Library for rules of use; OA articles are governed by the applicable Creative Commons License

Calassou, S., Larroque, C., & Malavieille, J. (1993). Transfer zones of deformation in thrust wedges: An experimental study. *Tectonophysics*, *221*(3–4), 325–344. https://doi.org/10.1016/0040-1951(93)90165-G

Calderon, Y., Baby, P., Hurtado, C., & Brusset, S. (2017). Thrust tectonics in the Andean retro-foreland basin of northern Peru: Permian inheritances and petroleum implications. *Marine and Petroleum Geology*, *82*, 238–250. https://doi.org/10.1016/j.marpetgeo.2017.02.009

Cazes, M., Torreilles, G., Bois, C., Damotte, B., Galdeano, A., Hirn, A., et al. (1985). Structure de la croute hercynienne du Nord de la France; premiers resultats du profil ECORS. *Bulletin de la Societe Geologique de France*, *1*(6), 925–941. https://doi.org/10.2113/gssgfbull.I.6.925

C.F.P.(M), COPESEP, R. A. P., & S. N. P. A. (1965). Contribution à la connaissance des bassins paléozoïques du Nord de la France. *Annales de la Societe Geologique du Nord*, *85*, 273–281.

Chantraine, J., Autran, A., Cavelier, C., Alabouvette, B., Barféty, J.-C., Cecca, F., et al. (2003). *Carte géologique de la France à l'échelle du millionième, 6^e édition révisée*. BRGM.

Chapple, W. M. (1978). Mechanics of thin-skinned fold-and-thrust belts. *GSA Bulletin*, *89*(8), 1189–1198. https://doi.org/10.1130/0016-7606(1978)89<1189:MOTFB>2.0.CO;2

Cobert, C., Baele, J.-M., Boulvais, P., Poujol, M., & Decrée, S. (2018). Petrogenesis of the Mairupt microgranite: A witness of an Uppermost Silurian magmatism in the Rocroi Inlier, Ardenne Allochton. *Comptes Rendus Geoscience*, *350*(3), 89–99. https://doi.org/10.1016/j.crte.2017.12.001

Coen-Aubert, M., Groessens, E., & Legrand, R. (1980). Les formations paléozoïques des sondages de Tournai et de Leuze. *Bulletin de la Société belge de Géologie*, *89*(4), 241–275.

Cook, B. S., & Thomas, W. A. (2009). Superposed lateral ramps in the Pell City thrust sheet, Appalachian thrust belt, Alabama. *Journal of Structural Geology*, *31*(9), 941–949. https://doi.org/10.1016/j.jsg.2009.06.001

Corfield, S. M., Gawthorpe, R. L., Gage, M., Fraser, A. J., & Besly, B. M. (1996). Inversion tectonics of the Variscan foreland of the British Isles. *Journal of the Geological Society*, *153*(1), 17–32. https://doi.org/10.1144/gsjgs.153.1.0017

Dahlen, F. A., Suppe, J., & Davis, D. (1984). Mechanics of fold-and-thrust belts and accretionary wedges: Cohesive Coulomb Theory. *Journal of Geophysical Research: Solid Earth*, *89*(B12), 10087–10101. https://doi.org/10.1029/JB089iB12p10087

Dahlstrom, C. D. A. (1969). Balanced cross sections. *Canadian Journal of Earth Sciences*, *6*(4), 743–757. https://doi.org/10.1139/e69-069

Davis, D., Suppe, J., & Dahlen, F. A. (1983). Mechanics of fold-and-thrust belts and accretionary wedges. *Journal of Geophysical Research: Solid Earth*, *88*(B2), 1153–1172. https://doi.org/10.1029/JB088iB02p01153

Debacker, T. N., Dewaele, S., Sintubin, M., Verniers, J., Muchez, P., & Boven, A. (2005). Timing and duration of the progressive deformation of the Brabant Massif, Belgium. *Geologica Belgica*, *8*(4), 20–34.

DeCelles, P. G., & Giles, K. A. (1996). Foreland basin systems. *Basin Research*, *8*(2), 105–123. https://doi.org/10.1046/j.1365-2117.1996.01491.x

Delmer, A. (1997). Structure tectonique du bassin houiller du Hainaut. *Annales de la Societe Geologique du Nord*, *5*(2), 7–15.

Delmer, A. (2003). La structure tectonique transfrontalière entre les bassins houillers de Valenciennes (France) et du Hainaut belge. *Geologica Belgica*, *6*(3–4), 171–180.

Delmer, A., Dusar, M., & Delcambre, B. (2001). Upper Carboniferous lithostratigraphic units (Belgium). *Geologica Belgica*, *4*(1–2), 95–103. https://doi.org/10.20341/gb.2014.045

Delmer, A., Leclercq, V., Marlière, R., & Robaszynski, F. (1982). La géothermie en Hainaut et le sondage de Ghlin (Mons - Belgique). *Annales de la Societe Geologique du Nord*, *101*, 189–206.

De Putter, T. (1995). Etude sédimentologique de la Grande brèche viséenne ("V3a") du bassin de Namur-Dinant. *Mém. Expl. Cartes Géologiques et Minières de la Belgique*, *40*, 1–272.

Dominguez, S., Malavieille, J., & Lallemand, S. E. (2000). Deformation of accretionary wedges in response to seamount subduction: Insights from sandbox experiments. *Tectonics*, *19*(1), 182–196. https://doi.org/10.1029/1999TC900055

Farquharson, N., Schubert, A., & Steiner, U. (2016). Geothermal Energy in Munich (and Beyond) A Geothermal City Case Study. *GRC Transactions*, *40*, 189–196.

Fielitz, W., & Mansy, J.-L. (1999). Pre- and synorogenic burial metamorphism in the Ardenne and neighboring areas (Rhenohercynian zone, central European Variscides). *Tectonophysics*, *309*(1–4), 227–256. https://doi.org/10.1016/S0040-1951(99)00141-9

Fillon, C., Huismans, R. S., & van der Beek, P. (2013). Syntectonic sedimentation effects on the growth of fold-and-thrust belts. *Geology*, *41*(1), 83–86. https://doi.org/10.1130/G33531.1

Fitz-Diaz, E., Hudleston, P., & Tolson, G. (2011). Comparison of tectonic styles in the Mexican and Canadian Rocky Mountain Fold-Thrust Belt. *Geological Society, London, Special Publications*, *349*(1), 149–167. https://doi.org/10.1144/SP349.8

Ford, M. (2004). Depositional wedge tops: Interaction between low basal friction external orogenic wedges and flexural foreland basins. *Basin Research*, *16*(3), 361–375. https://doi.org/10.1111/j.1365-2117.2004.00236.x

Franke, W. (1992). Phanerozoic structures and events in Central Europe. In D. Blundell, R. Freeman, & S. Mueller (Eds.), *A continent revealed: The European geotraverse* (pp. 164–179). Cambridge University Press.

Franke, W. (2000). The mid-European segment of the Variscides: Tectonostratigraphic units, terrane boundaries and plate tectonic evolution. *Geological Society, London, Special Publications*, *179*(1), 35–61. https://doi.org/10.1144/GSL.SP.2000.179.01.05

Franke, W. (2006). The Variscan orogen in Central Europe: Construction and collapse. *Geological Society, London, Memoirs*, *32*(1), 333–343. https://doi.org/10.1144/GSL.MEM.2006.032.01.20

Franke, W., Cocks, L. R. M., & Torsvik, T. H. (2017). The Palaeozoic Variscan oceans revisited. *Gondwana Research*, *48*, 257–284. https://doi.org/10.1016/j.gr.2017.03.005

Franke, W., Dallmeyer, R. D., & Weber, K. (1995). Geodynamic Evolution. In R. D. Dallmeyer, W. Franke, & K. Weber (Eds.), *Pre-permian geology of central and eastern Europe* (pp. 579–593). Springer-Verlag. https://doi.org/10.1007/978-3-642-77518-5_57

Frizon de Lamotte, D., Guezou, J.-C., & Averbuch, O. (1995). Distinguishing lateral folds in thrust-systems; examples from Corbières (SW France) and Betic Cordilleras (SE Spain). *Journal of Structural Geology*, *17*(2), 233–244. https://doi.org/10.1016/0191-8141(94)e0035-w

Gillcrist, R., Coward, M., & Mugnier, J.-L. (1987). Structural inversion and its controls: Examples from the Alpine foreland and the French Alps. *Geodinamica Acta*, *1*(1), 5–34. https://doi.org/10.1080/09853111.1987.11105122

Golonka, J. (2002). Plate-Tectonic Maps of the Phanerozoic. *SEPM Special Publications*, *72*, 21–75. https://doi.org/10.2110/pec.02.72.0021

Golonka, J. (2020). Late Devonian paleogeography in the framework of global plate tectonics. *Global and Planetary Change*, *186*, 103129. https://doi.org/10.1016/j.gloplacha.2020.103129

Golonka, J., & Gawęda, A. (2012). Plate Tectonic Evolution of the Southern Margin of Laurussia in the Paleozoic. In E. Sharkov (Ed.), *Tectonics-Recent advances* (pp. 261–282). InTech. https://doi.org/10.5772/50009

Graveleau, F., Malavieille, J., & Dominguez, S. (2012). Experimental modeling of orogenic wedges: A review. *Tectonophysics*, *538–540*, 1–66. https://doi.org/10.1016/j.tecto.2012.01.027

19449194, 2021, 7, Downloaded from https://agupubs.onlinelibrary.wiley.com/doi/10.1029/2020TC006642 by Cochrane France, Wiley Online Library on [13/12/2023]. See the Terms and Conditions (https://onlinelibrary.wiley.com/terms-and-conditions) on Wiley Online Library for rules of use; OA articles are governed by the applicable Creative Commons License

Guillot, F., Averbuch, O., Dubois, M., Durand, C., Lanari, P., & Gauthier, A. (2020). Zircon age of vaugnerite intrusives from the Central and Southern Vosges crystalline massif (E France): Contribution to the geodynamics of the European Variscan belt. *BSGF - Earth Sciences Bulletin*, *191*, 26. https://doi.org/10.1051/bsgf/2020027

Gutscher, M.-A., Kukowski, N., Malavieille, J., & Lallemand, S. (1996). Cyclical behavior of thrust wedges: Insights from high basal friction sandbox experiments. *Geology*, *24*(2), 135–138. https://doi.org/10.1130/0091-7613(1996)024<0135:CBOTWI>2.3.CO;2

Hammerstein, J. A., Di Cuia, R., Cottam, M. A., Zamora, G., & Butler, R. W. H. (2020). *Fold and thrust belts: Structural Style, Evolution and Exploration*. Geological Society, London, Special Publications. 490(1). https://doi.org/10.1144/SP490

Hance, L., Dejonghe, L., Ghysel, P., Laloux, M., & Mansy, J.-L. (1999). Influence of heterogeneous lithostructural layering on orogenic deformation in the Variscan Front Zone (eastern Belgium). *Tectonophysics*, *309*(1–4), 161–177. https://doi.org/10.1016/S0040-1951(99)00137-7

Hance, L., & Poty, E. (2006). Hastarian. *Geologica Belgica*, *9*(1–2), 111–116.

Houchen, M. A. (1988). *Structural modeling of the external Variscides of France and Belgium (Doctoral dissertation)*. National University of Ireland.

Hughes, A. (2020). Mechanical controls on structural styles in shortening environments: A discrete-element modeling approach. *Geological Society, London, Special Publications*, *490*(1), 33–55. https://doi.org/10.1144/SP490-2019-114

Huiqi, L., McClay, K. R., & Powell, D. (1992). Physical models of thrust wedges. In K. R. McClay (Ed.), *Thrust tectonics* (pp. 71–81). Springer. https://doi.org/10.1007/978-94-011-3066-0_6

Jones, P. B. (1982). Oil and gas beneath east-dipping underthrust faults in the Alberta Foothills, Canada. *Geological Studies of the Cordilleran Thrust Belt*, *1*, 61–74.

Karner, G. D., & Watts, A. B. (1983). Gravity anomalies and flexure of the lithosphere at mountain ranges. *Journal of Geophysical Research: Solid Earth*, *88*(B12), 10449–10477. https://doi.org/10.1029/JB088iB12p10449

Khatir, A., Mansy, J.-L., & Meilliez, F. (1988). Structures et déformation dans l'allochtone ardennais en Avesnois (Nord). *Annales de la Societe Geologique du Nord*, *108*(2–3), 73–83.

Khatir, A., Mansy, J.-L., & Meilliez, F. (1992). Structuration varisque en Ardenne occidentale: Une hiérarchie des niveaux de décollement. *Comptes rendus de l'Académie des sciences. Série 2. Mécanique, Physique, Chimie, Sciences de l'univers, Sciences de La Terre*, *314*(4), 365–371.

Kley, J., Monaldi, C. R., & Salfity, J. A. (1999). Along-strike segmentation of the Andean foreland: Causes and consequences. *Tectonophysics*, *301*(1–2), 75–94. https://doi.org/10.1016/S0040-1951(98)90223-2

Konstantinovskaya, E., & Malavieille, J. (2005). Accretionary orogens: Erosion and exhumation. *Geotectonics*, *39*(1), 69–86.

Konstantinovskaya, E., Malo, M., & Badina, F. (2014). Effects of irregular basement structure on the geometry and emplacement of frontal thrusts and duplexes in the Quebec Appalachians: Interpretations from well and seismic reflection data. *Tectonophysics*, *637*, 268–288. https://doi.org/10.1016/j.tecto.2014.10.012

Krzywiec, P., Mazur, S., Gagala, L., Kufrasa, M., Lewandowski, M., Malinowski, M., & Buffenmyer, V. (2017). Late Carboniferous thin-skinned compressional deformation above the SW edge of the East European craton as revealed by seismic reflection and potential field data–Correlations with the Variscides and the Appalachians. In R. D. Law, J. R. Thigpen, A. J. Merschat, & H. H. Stowell (Eds.), Linkages and Feedbacks in orogenic systems (Vol. 213, pp. 20). Geological Society of America Memoir. https://doi.org/10.1130/2017.1213(14

Kufrasa, M., Krzywiec, P., Gagala, L., Mazur, S., & Mikolajczak, M. (2020). Sequence of deformation at the front of an orogen: Lublin basin case study (Poland). *Journal of Structural Geology*, *141*, 1–18. https://doi.org/10.1016/j.jsg.2020.104211

Lacombe, O., Lavé, J., Roure, F. M., & Verges, J. (2007). *Thrust belts and foreland basins - from fold kinematics to hydrocarbon systems*. Springer-Verlag. https://doi.org/10.1007/978-3-540-69426-7

Lacombe, O., & Mouthereau, F. (2002). Basement-involved shortening and deep detachment tectonics in forelands of orogens: Insights from recent collision belts (Taiwan, Western Alps, Pyrenees). *Tectonics*, *21*(4), 12–22. https://doi.org/10.1029/2001TC901018

Lacombe, O., Mouthereau, F., Angelier, J., Chu, H.-T., & Lee, J.-C. (2003). Frontal belt curvature and oblique ramp development at an obliquely collided irregular margin: Geometry and kinematics of the NW Taiwan fold-thrust belt. *Tectonics*, *22*(3), 1–16. https://doi.org/10.1029/2002TC001436

Lacquement, F. (2001). *L'Ardenne Varisque. Déformation progressive d'un prisme sédimentaire pré-structuré, de l'affleurement au modèle de chaîne. (Publication No. 29)*. Société Géologique du Nord.

Lacquement, F., Averbuch, O., Mansy, J.-L., Szaniawski, R., & Lewandowski, M. (2005). Transpressional deformations at lateral boundaries of propagating thrust-sheets: The example of the Meuse Valley Recess within the Ardennes Variscan fold-and-thrust belt (N France–S Belgium). *Journal of Structural Geology*, *27*(10), 1788–1802. https://doi.org/10.1016/j.jsg.2005.05.017

Lacquement, F., Mansy, J.-L., Hanot, F., & Meilliez, F. (1999). Retraitement et interprétation d'un profil sismique pétrolier méridien au travers du Massif paléozoïque ardennais (Nord de la France). *Comptes Rendus de l'Academie des Sciences-Series IIA: Earth and Planetary Science*, *329*(7), 471–477. https://doi.org/10.1016/S1251-8050(00)80020-8

Lallemand, S. E., Malavieille, J., & Calassou, S. (1992). Effects of oceanic ridge subduction on accretionary wedges: Experimental modeling and marine observations. *Tectonics*, *11*(6), 1301–1313. https://doi.org/10.1029/92TC00637

Le Gall, B. (1992). The deep structure of the Ardennes Variscan thrust belt from structural and ECORS seismic data. *Journal of Structural Geology*, *14*(5), 531–546. https://doi.org/10.1016/0191-8141(92)90155-P

Le Gall, B. (1994). Deformation of the Nord-Pas-de-Calais Carboniferous Coalfield (France) in the Variscan Frontal Tectonic Pattern. In A. Mascle (Ed.), Hydrocarbon and Petroleum geology of France. Special Publication of the European Association of Petroleum Geoscientists (Vol. 4, pp. 379–398). Springer-Verlag. https://doi.org/10.1007/978-3-642-78849-9_27

Legeay, E., Ringenbach, J.-C., Kergaravat, C., Pichat, A., Mohn, G., Vergés, J., et al. (2020). Structure and kinematics of the Central Sivas Basin (Turkey): Salt deposition and tectonics in an evolving fold-and-thrust belt. *Geological Society, London, Special Publications*, *490*(1), 361–396. https://doi.org/10.1144/SP490-2019-92

Legrand, R. (1968). Le Massif du Brabant. *Mémoires pour servir à l'Explication des Cartes Géologiques et Minières de la Belgique*, *9*, 1–148.

Leveridge, B. E. (2011). The Looe, South Devon and Tavy basins: The Devonian rifted passive margin successions. *Proceedings of the Geologists' Association*, *122*(4), 616–717. https://doi.org/10.1016/j.pgeola.2011.03.005

Licour, L. (2012). Relations entre la géologie profonde et le comportement hydrogéologique du réservoir géothermique du Hainaut (Belgique) - Caractérisation de l'aquifère dans la région de Saint-Ghislain (Doctoral dissertation). Mons, Belgium: Université de Mons.

Malavieille, J. (2010). Impact of erosion, sedimentation, and structural heritage on the structure and kinematics of orogenic wedges: Analog models and case studies. *Geological Society of America Today*, *20*(1), 4–10. https://doi.org/10.1130/GSATG48A.1

Malz, A., Madritsch, H., Jordan, P., Meier, B., & Kley, J. (2020). Along-strike variations in thin-skinned thrusting style controlled by pre-existing basement structure in the easternmost Jura Mountains (Northern Switzerland). *Geological Society, London, Special Publications*, *490*(1), 199–220. https://doi.org/10.1144/SP490-2019-090

19449194, 2021, 7, Downloaded from https://agupubs.onlinelibrary.wiley.com/doi/10.1029/2020TC006642 by Cochrane France, Wiley Online Library on [13/12/2023]. See the Terms and Conditions (https://onlinelibrary.wiley.com/terms-and-conditions) on Wiley Online Library for rules of use; OA articles are governed by the applicable Creative Commons License

Mansy, J. L., Everaerts, M., & De Vos, W. (1999). Structural analysis of the adjacent Acadian and Variscan fold belts in Belgium and northern France from geophysical and geological evidence. *Tectonophysics*, *309*(1–4), 99–116. https://doi.org/10.1016/S0040-1951(99)00134-1

Mansy, J.-L., & Lacquement, F. (2006). Contexte géologique régional: L'Ardenne paléozoïque (Nord de la France et Sud de la Belgique). *Géologie de la France*, *1–2*, 7–13.

Mansy, J.-L., Lacquement, F., Meilliez, F., Hanot, F., & Everaerts, M. (1997). Interprétation d'un profil sismique pétrolier, sur le méridien de Valenciennes (Nord de la France). *Aardkundige Mededelingen*, *8*, 127–129.

Mansy, J.-L., Manby, G. M., Averbuch, O., Everaerts, M., Bergerat, F., Van Vliet-Lanoe, B., et al. (2003). Dynamics and inversion of the Mesozoic Basin of the Weald–Boulonnais area: Role of basement reactivation. *Tectonophysics*, *373*(1–4), 161–179. https://doi.org/10.1016/S0040-1951(03)00289-0

Mansy, J.-L., & Meilliez, F. (1993). Eléments d'analyse structurale à partir d'exemples pris en Ardenne-Avesnois. *Annales de la Societe Geologique du Nord*, *2*(2), 45–60.

Marshak, S. (2004). Salients, Recesses, Arcs, Oroclines, and Syntaxes—A Review of Ideas Concerning the Formation of Map-view Curves in Fold-thrust Belts. In K. R. McClay (Ed.), Thrust Tectonics and Hydrocarbon systems (Vol. 82, pp. 131–156).

Martinez, A., Malavieille, J., Lallemand, S., & Collot, J.-Y. (2002). Strain partitioning in an accretionary wedge, in oblique convergence: Analogue modeling. *Bulletin de La Société Géologique de France*, *173*(1), 17–24. https://doi.org/10.2113/173.1.17

Matte, P. (2001). The Variscan collage and orogeny (480-290 Ma) and the tectonic definition of the Armorica microplate: A review. *Terra Nova*, *13*(2), 122–128. https://doi.org/10.1046/j.1365-3121.2001.00327.x

Mazur, S., Aleksandrowski, P., Gagala, L., Krzywiec, P., Zaba, J., Gaidzik, K., & Sikora, R. (2020). Late Palaeozoic strike-slip tectonics versus oroclinal bending at the SW outskirts of Baltica: Case of the Variscan belt's eastern end in Poland. *International Journal of Earth Sciences*, *109*(4), 1133–1160. https://doi.org/10.1007/s00531-019-01814-7

McClay, K. R. (1992). Glossary of thrust tectonics terms. In K. R. McClay (Ed.), *Thrust tectonics* (pp. 419–433). Springer Science & Business Media.

McClay, K. R. (2004). Thrust Tectonics and Hydrocarbon Systems (Vol. 82, pp. 667). AAPG Memoir. https://doi.org/10.1306/M82813

McClay, K. R., Whitehouse, P. S., Dooley, T., & Richards, M. (2004). 3D evolution of fold and thrust belts formed by oblique convergence. *Marine and Petroleum Geology*, *21*(7), 857–877. https://doi.org/10.1016/j.marpetgeo.2004.03.009

Meilliez, F. (1989).Importance de l'événement calédonien dans l'allochtone ardennais; essai sur une cinématique paléozoïque de l'Ardenne dans la chaîne Varisque (Doctoral dissertation). Le Mans, France: Université du Maine.

Meilliez, F. (2019). La Faille du Midi, mythe et réalités. *Annales de la Societe Geologique du Nord*, *26*(2), 13–32.

Meilliez, F., André, L., Blieck, A., Fielitz, W., Goffette, O., Hance, L., et al. (1991). Ardenne-Brabant. *Sciences Géologiques. Bulletin*, *44*(1–2), 3–29. https://doi.org/10.3406/sgeol.1991.1864

Meilliez, F., & Mansy, J. L. (1990). Déformation pelliculaire différenciée dans une série lithologique hétérogène ; le Dévono-Carbonifère de l'Ardenne. *Bulletin de la Societe Geologique de France*, *6*(1), 177–188. https://doi.org/10.2113/gssgfbull.VI.1.177

Minguely, B., Averbuch, O., Patin, M., Rolin, D., Hanot, F., & Bergerat, F. (2010). Inversion tectonics at the northern margin of the Paris basin (northern France): New evidence from seismic profiles and boreholes interpolation in the Artois area. *Bulletin de la Societe Geologique de France*, *181*(5), 429–442. https://doi.org/10.2113/gssgfbull.181.5.429

Minguely, B., Folens, L., Averbuch, O., & Vendeville, B. C. (2008). Formation of deep-seated triangle zones by interaction between two orogenic thrust fronts having opposite vergence: Structural evidence from the Caledonian-Variscan system in Northern France and preliminary analogue modeling. *Bollettino Di Geofisica*, *49*(2), 242–246.

Moore, J. C. (1989). Tectonics and hydrogeology of accretionary prisms: Role of the décollement zone. *Journal of Structural Geology*, *11*(1–2), 95–106. https://doi.org/10.1016/0191-8141(89)90037-0

Morley, C. K. (1986). A Classification of Thrust Fronts. *AAPG Bulletin*, *70*(1), 12–25. https://doi.org/10.1306/94885615-1704-11d7-8645000102c1865d

Morley, C. K. (1988). Out-of-Sequence Thrusts. *Tectonics*, *7*(3), 539–561. https://doi.org/10.1029/TC007i003p00539

Mortelmans, G., & Bourguignon, P. (1954). *Partie 1. La stratigraphie. Chapitre 6Le Dinantien*. Annales de la Société géologique de Belgique, Special publications: Prodrome d'une description géologique de la Belgique, (pp. 217–321).

Moulouel, H. (2008). Caractérisation cartographique d'une différenciation verticale et horizontale de la déformation: Application à la couverture sédimentaire de la plate-forme ardennaise. (Doctoral dissertation). Lille, France: Université des Sciences et Technologies de Lille.

Needham, D. T., Matthews, S. J., & Butler, R. W. H. (2004). Oil and Gas in Compressional Belts. *Marine and Petroleum Geology*, *21*(7), 783–964. https://doi.org/10.1016/j.marpetgeo.2004.04.002

Nemcok, M., Schamel, S., & Gayer, R. (2005). *Thrustbelts: Structural architecture, thermal regimes and petroleum systems*. Cambridge University Press. https://doi.org/10.1017/CBO9780511584244

Oncken, O., Plesch, A., Weber, J., Ricken, W., & Schrader, S. (2000). Passive margin detachment during arc-continent collision (Central European Variscides). *Geological Society, London, Special Publications*, *179*(1), 199–216. https://doi.org/10.1144/GSL.SP.2000.179.01.13

Oncken, O., von Winterfeld, C., & Dittmar, U. (1999). Accretion of a rifted passive margin: The Late Paleozoic Rhenohercynian fold and thrust belt (Middle European Variscides). *Tectonics*, *18*(1), 75–91. https://doi.org/10.1029/98TC02763

Ortner, H., Aichholzer, S., Zerlauth, M., Pilser, R., & Fügenschuh, B. (2015). Geometry, amount, and sequence of thrusting in the Subalpine Molasse of western Austria and southern Germany, European Alps: Thrusting in the Alpine Foreland. *Tectonics*, *34*(1), 1–30. https://doi.org/10.1002/2014TC003550

Paulsen, T., & Marshak, S. (1999). Origin of the Uinta recess, Sevier fold–thrust belt, Utah: Influence of basin architecture on fold–thrust belt geometry. *Tectonophysics*, *312*(2), 203–216. https://doi.org/10.1016/S0040-1951(99)00182-1

Pharaoh, T. (2018). The Anglo-Brabant Massif: Persistent but enigmatic palaeo-relief at the heart of western Europe. *Proceedings of the Geologists' Association*, *129*(3), 278–328. https://doi.org/10.1016/j.pgeola.2018.02.009

Pharaoh, T. C., Molyneux, S. G., Merriman, R. J., Lee, M. K., & Verniers, J. (1993). The Caledonides of the Anglo-Brabant Massif reviewed. *Geological Magazine*, *130*(5), 561–562. https://doi.org/10.1017/S0016756800020847

Plesch, A., & Oncken, O. (1999). Orogenic wedge growth during collision—constraints on mechanics of a fossil wedge from its kinematic record (Rhenohercynian FTB, Central Europe). *Tectonophysics*, *309*(1–4), 117–139. https://doi.org/10.1016/S0040-1951(99)00135-3

Poblet, J., & Lisle, R. J. (2011). Kinematic Evolution and Structural Styles of Fold-and-Thrust Belts. *Geological Society, London, Special Publications*, *349*(1). https://doi.org/10.1144/SP349.1

Poty, E., Hance, L., Lees, A., & Hennebert, M. (2001). Dinantian lithostratigraphic units (Belgium). *Geologica Belgica*, *4*(1–2), 69–94. https://doi.org/10.20341/gb.2014.044

19449194, 2021, 7, Downloaded from https://agupubs.onlinelibrary.wiley.com/doi/10.1029/2020TC006642 by Cochrane France, Wiley Online Library on [13/12/2023]. See the Terms and Conditions (https://onlinelibrary.wiley.com/terms-and-conditions) on Wiley Online Library for rules of use; OA articles are governed by the applicable Creative Commons License

Préat, A., & Boulvain, F. (1988). Excursion A-1. Middle and Upper Devonian carbonate platform evolution in Dinant and Namur basins (Belgium, France). In A. Herbosch (Ed.), *IAS 9th European regional meeting: Excursion guidebook leuven-Belgium* (p. 1–25). Belgium: Ministery of Economic Affairs, Belgian Geological Survey.

Price, R. A. (1986). The southeastern Canadian Cordillera: Thrust faulting, tectonic wedging, and delamination of the lithosphere. *Journal of Structural Geology*, *8*(3–4), 239–254. https://doi.org/10.1016/0191-8141(86)90046-5

Qayyum, M., Spratt, D. A., Dixon, J. M., & Lawrence, R. D. (2015). Displacement transfer from fault-bend to fault-propagation fold geometry: An example from the Himalayan thrust front. *Journal of Structural Geology*, *77*, 260–276. https://doi.org/10.1016/j.jsg.2014.10.010

Raoult, J.-F. (1986). Le front varisque du Nord de la France d'après les profils sismiques, la géologie de surface et les sondages. *Revue de Geologie Dynamique et de Geographie Physique*, *27*(3–4), 247–268.

Raoult, J.-F. (1988). Le front varisque du Nord de la France: Interprétation des principales coupes d'après les profils sismiques, la géologie de surface et les sondages. In M. Cazes, & G. Torreilles (Eds.), *Etude de la croûte terrestre par sismique profonde: Profil du Nord de la France* (pp. 171–196). Technip.

Raoult, J.-F., & Meilliez, F. (1987). The variscan front and the midi fault between the channel and the meuse river. *Journal of Structural Geology*, *9*(4), 473–479. https://doi.org/10.1016/0191-8141(87)90122-2

Ravaglia, A., Seno, S., Toscani, G., & Fantoni, R. (2006). Mesozoic extension controlling the Southern Alps thrust front geometry under the Po Plain, Italy: Insights from sandbox models. *Journal of Structural Geology*, *28*(11), 2084–2096. https://doi.org/10.1016/j.jsg.2006.07.011

Rouchy, J. M., Laumondais, A., & Groessens, E. (1987). The lower Carboniferous (Visean) evaporites in northern France and Belgium: Depositional, diagenetic and deformational guides to reconstruct a disrupted evaporitic basin. In T. M. Peryt (Ed.), *Evaporite basins* (Vol. 13, pp. 31–67). Springer-Verlag. https://doi.org/10.1007/BFb0010099

Rouchy, J. M., Pierre, C., Groessens, E., Monty, C., Laumondais, A., & Moine, B. (1986). Les évaporites pré-permiennes du segment varisque franco-belge: Aspects paléogéographiques et structuraux. *Bulletin de la Société belge de Géologie*, *95*(2–3), 139–149.

Schedl, A., & Wiltschko, D. V. (1987). Possible effects of pre-existing basement topography on thrust fault ramping. *Journal of Structural Geology*, *9*(8), 1029–1037. https://doi.org/10.1016/0191-8141(87)90011-3

Schulmann, K., Schaltegger, U., Jezek, J., Thompson, A. B., & Edel, J.-B. (2002). Rapid burial and exhumation during orogeny: Thickening and synconvergent exhumation of thermally weakened and thinned crust (Variscan orogen in Western Europe). *American Journal of Science*, *302*(10), 856–879. https://doi.org/10.2475/ajs.302.10.856

Scisciani, V. (2009). Styles of positive inversion tectonics in the Central Apennines and in the Adriatic foreland: Implications for the evolution of the Apennine chain (Italy). *Journal of Structural Geology*, *31*(11), 1276–1294. https://doi.org/10.1016/j.jsg.2009.02.004

Shail, R. K., & Leveridge, B. E. (2009). The Rhenohercynian passive margin of SW England: Development, inversion and extensional reactivation. *Comptes Rendus Geoscience*, *341*(2–3), 140–155. https://doi.org/10.1016/j.crte.2008.11.002

Sintubin, M., Debacker, T. N., & Van Baelen, H. (2009). Early Palaeozoic orogenic events north of the Rheic suture (Brabant, Ardenne): A review. *Comptes Rendus Geoscience*, *341*(2), 156–173. https://doi.org/10.1016/j.crte.2008.11.012

Smeraglia, L., Fabbri, O., Choulet, F., Buatier, M., Boulvais, P., Bernasconi, S. M., & Castorina, F. (2020). Syntectonic fluid flow and deformation mechanisms within the frontal thrust of a foreland fold-and-thrust belt: Example from the Internal Jura, Eastern France. *Tectonophysics*, *778*, 1–21. https://doi.org/10.1016/j.tecto.2019.228178

Smit, J., van Wees, J.-D., & Cloetingh, S. (2018). Early Carboniferous extension in East Avalonia: 350 My record of lithospheric memory. *Marine and Petroleum Geology*, *92*, 1010–1027. https://doi.org/10.1016/j.marpetgeo.2018.01.004

Storti, F., & McClay, K. (1995). Inuence of syntectonic sedimentation on thrust wedges in analogue models. *Geology*, *23*(11), 999–1002. https://doi.org/10.1130/0091-7613(1995)023<0999:iossot>2.3.co;2

Suppe, J. (1983). Geometry and kinematics of fault-bend folding. *American Journal of Science*, *283*(7), 684–721. https://doi.org/10.2475/ajs.283.7.684

Szaniawski, R., Lewandowski, M., Mansy, J.-L., Averbuch, O., & Lacquement, F. (2003). Syn-folding remagnetization events in the French-Belgium Variscan thrust front as markers of the fold-and-thrust belt kinematics. *Bulletin de la Societe Geologique de France*, *174*(5), 511–523. https://doi.org/10.2113/174.5.511

Tanner, D. C., Bense, F. A., & Ertl, G. (2011). Kinematic retro-modeling of a cross-section through a thrust-and-fold belt: The Western Irish Namurian Basin. *Geological Society, London, Special Publications*, *349*(1), 61–76. https://doi.org/10.1144/SP349.4

Tavarnelli, E. (1996). The effects of preexisting normal faults on thrust ramp development: An example from the northern Apennines, Italy. *Geologische Rundschau*, *85*, 363–371. https://doi.org/10.1007/BF02422241

Tavarnelli, E. (1999). Normal faults in thrust sheets: Pre-orogenic extension, post-orogenic extension, or both? *Journal of Structural Geology*, *21*(8–9), 1011–1018. https://doi.org/10.1016/S0191-8141(99)00034-6

Thomas, W. A. (2001). Mushwad: Ductile duplex in the Appalachian thrust belt in Alabama. *AAPG Bulletin*, *85*(10), 1847–1869. https://doi.org/10.1306/8626D08B-173B-11D7-8645000102C1865D

Thomas, W. A. (2007). Role of the Birmingham basement fault in thin-skinned thrusting of the Birmingham anticlinorium, Appalachian thrust belt in Alabama. *American Journal of Science*, *307*(1), 46–62. https://doi.org/10.2475/01.2007.03

Thorez, J., & Dreesen, R. (1986). A model of a regressive depositional system around the Old Red Continent as exemplified by a field trip in the Upper Famennian "Psammites du Condroz" in Belgium. *Annales de la Société Géologique de Belgique*, *109*, 285–323.

Toscani, G., Bonini, L., Ahmad, M. I., Di Bucci, D., Di Giulio, A., Seno, S., & Galuppo, C. (2014). Opposite verging chains sharing the same foreland: Kinematics and interactions through analogue models (Central Po Plain, Italy). *Tectonophysics*, *633*, 268–282. https://doi.org/10.1016/j.tecto.2014.07.019

Tozer, R. S. J., Butler, R. W. H., Chiappini, M., Corrado, S., Mazzoli, S., & Speranza, F. (2006). Testing thrust tectonic models at mountain fronts: Where has the displacement gone? *Journal of the Geological Society*, *163*, 1–14. https://doi.org/10.1144/0016-764904-140

Ustaszewski, K., & Schmid, S. M. (2006). Control of preexisting faults on geometry and kinematics in the northernmost part of the Jura fold-and-thrust belt. *Tectonics*, *25*, 1–26. https://doi.org/10.1029/2005TC001915

Van Grootel, G., Verniers, J., Geerkens, B., Laduron, D., Verhaeren, M., Hertogen, J., & De Vos, W. (1997). Timing of magmatism, foreland basin development, metamorphism and inversion in the Anglo-Brabant fold belt. *Geological Magazine*, *134*(5), 607–616. https://doi.org/10.1017/S0016756897007413

Van Hulten, F. F. N. (2012). Devono-Carboniferous carbonate platform systems of the Netherlands. *Geologica Belgica*, *15*(4), 284–296.

Vann, I. R., Graham, R. H., & Hayward, A. B. (1986). The structure of mountain fronts. *Journal of Structural Geology*, *8*(3–4), 215–227. https://doi.org/10.1016/0191-8141(86)90044-1

Verniers, J., Herbosch, A., Vanguestaine, M., Geukens, F., Delcambre, B., Pingot, J.-L., et al. (2001). Cambrian-Ordovician-Silurian lithostratigraphic units (Belgium). *Geologica Belgica*, *4*(1–2), 5–38.

19449194, 2021, 7, Downloaded from https://agupubs.onlinelibrary.wiley.com/doi/10.1029/2020TC006642 by Cochrane France, Wiley Online Library on [13/12/2023]. See the Terms and Conditions (https://onlinelibrary.wiley.com/terms-and-conditions) on Wiley Online Library for rules of use; OA articles are governed by the applicable Creative Commons License

Von Hagke, C., & Malz, A. (2018). Triangle zones–Geometry, kinematics, mechanics, and the need for appreciation of uncertainties. *Earth-Science Reviews*, *177*, 24–42. https://doi.org/10.1016/j.earscirev.2017.11.003

Wiltschko, D., & Eastman, D. (1983). Role of basement warps and faults in localizing thrust fault ramps. In R. D. Hatcher, Jr, H. Williams, & I. Zietz (Eds.), Contributions to the Tectonics and Geophysics of Mountain Chains (Vol. 158, pp. 177–190). GSA Memoirs. https://doi.org/10.1130/mem158-p177

Wu, J. E., & McClay, K. R. (2011). Two-dimensional Analog Modeling of Fold and Thrust Belts: Dynamic Interactions with Syncontractional Sedimentation and Erosion. In K. R. McClay, J. H. Shaw, & J. Suppe (Eds.), Thrust Fault-Related Folding (Vol. 94, pp. 301–333). AAPG Memoir.

Ziegler, P. A. (1989). *Evolution of Laurussia: A study in late palaeozoic plate tectonics*. Kluwer Academic Publishers. https://doi.org/10.1007/978-94-009-0469-9

Ziegler, P. A. (1990). *Geological atlas of western and central Europe*. Shell Internationale Petroleum Maatschappij B.V.

Ziegler, P. A., Bertotti, G., & Cloetingh, S. (2002). Dynamic processes controlling foreland development - The role of mechanical (de)coupling of orogenic wedges and forelands. *Stephan Mueller Special Publication Series*, *1*, 17–56. https://doi.org/10.5194/smsps-1-17-2002

19449194, 2021, 7, Downloaded from https://agupubs.onlinelibrary.wiley.com/doi/10.1029/2020TC006642 by Cochrane France, Wiley Online Library on [13/12/2023]. See the Terms and Conditions (https://onlinelibrary.wiley.com/terms-and-conditions) on Wiley Online Library for rules of use; OA articles are governed by the applicable Creative Commons License